REVIEW ARTICLE

Influence of activation conditions on the physicochemical properties of activated biochar: a review

N. L. Panwar[1] · Ashish Pawar[1]

Abstract

The biochar produced from agricultural crop residues through thermochemical processes helps in crop waste management. Biochar has paid more attention due to its distinctive features such as high organic carbon content, stable structure, large surface area, and cation exchange capacity. The biochar obtained from crop residues can be readily converted into activated biochar. This review paper systematically summarised the preparation of activated biochar, characterisation, and analytical techniques of activated biochar based on more than 150 literatures published in the last 10 years. The physicochemical properties of activated biochar varies according to the type of feedstock, pyrolysis condition, and mode of activation. The selection of the activation method mainly depends on its further end environmental application. Physical activation or steam purging at high temperature creates pores inside biochar. Gas purging increases the surface area and pore volume, although steam activation is not much suitable to improve the BC surface functionality as compared to chemical and impregnation activation. Sulphuric and oxalic acid–modified biochar was found to be most suitable for the soil amendment. Alkaline activation enhances the surface area and oxygen-containing functional group in activated biochar. Metal oxide–modified biochar had better surface functionalities than did physical- and chemical-activated biochar and better sorption of organic and inorganic contaminants from potable water and waste water. In summary, activated biochar has a wide environmental prospect in remediation.

Keywords Biomass · Activated biochar · Activation methods · Impregnation techniques · Water purification

1 Introduction

Biochar (BC) is a stable, organic carbon (C)–rich by-product that is produced through biomass pyrolysis at elevated temperatures in oxygen-limited environments [1]. BC is recognised to be a multifunctional organic material, due to promising widespread applications, such as use as a soil amendment, C-sequestration, and the immobilisation of organic and inorganic contaminants [2]. These applications vary according to the physicochemical properties of the BC, which depend on the precursor type and pyrolysis conditions, including the reactor type, heating rate, residence time, and pyrolysis temperature. Among these operating conditions, the pyrolysis temperature plays a significant role when determining the end quality and applicability of BC. In general, BC produced at high pyrolysis temperatures (600–700 °C) has a highly aromatic nature, with a well-structured carbon layer; however, due to deoxygenation and dehydration, BC produced at high temperatures contains fewer oxygen- and hydrogen-containing functional groups, on its surface [3] and this type of BC possesses a low ion exchange capacity. In contrast, most BC produced at lower pyrolysis temperatures (300–400 °C) shows more diversified characteristics, including increased C, H, and C=O functional groups along with cellulosic and aliphatic structures [4]. BC produced at high pyrolysis temperatures presents an excellent platform for further activation and it has been applied to contaminant removal, through sorption processes [5].

Activated or modified BC can be prepared when raw BC is further activated to enhance the surface area, pore structure, and functionality. However, raw BC may exhibit a limited capacity for the sorption of specific contaminants in strong concentrations [6]. Activated BC, with improved surface functional groups, showed excellent sorption capacity; for example, MgO-activated pine wood–derived activated BC

✉ Ashish Pawar
  pawarashishraje123@gmail.com

1 Department of Renewable Energy Engineering, College of Technology and Engineering, Maharana Pratap University of Agriculture and Technology, Udaipur, Rajasthan 313001, India

demonstrated a 5-fold increase in Pb (II) sorption capacity compared with pristine BC [7]. Consequently, various activation processes are available, including physical activation, chemical activation, and impregnation techniques, which may improve the performance of BC during environmental remediation [8]. According to various researchers, activated BC can be employed as an alternative to activated carbon, carbon nanotubes and graphene, which have similar sorption capacities for various contaminants, likely due to the availability of surface functional groups in activated BC, such as carboxyl, carbonyl and hydroxyl groups and the atomic ratios of O/C, N/C and H/C [9]. In general, heat treatment, steam activation, chemical activation and impregnation techniques can enrich the surface functional groups on activated BC. Presently, activated BC represents a reliable alternative sorbent to activated carbon, carbon nanotubes and graphene, with similar adsorption capacities for organic and inorganic contaminants. Thus, the major benefits of activated biochar preparation are to overcome the waste-related problems, and the necessity of activated biochar tends towards the removal of heavy metals from waste water, also removal of anions, and organic and inorganic contaminants from aqueous solution. Specifically, the primary focus of this review paper is the thorough examination of recently published studies describing the preparation methodologies used to prepare activated BC and the improved physicochemical properties of BC following the various activation processes.

1.1 Importance of activated biochar

The biochar produced from biomass through thermochemical processes is often activated or modified using different activation methods including physical, chemical and impregnation methods to improve its surface area and porous structure and to form functional groups on the biochar surface prior to its environmental application (known as activated biochar) [10]. The thermochemical conversion of biomass produces biochar, having a polycyclic aromatic structure due to its carbon base. Therefore, it is economically feasible, carbon-neutral and environmentally friendly [11]. Since biochar is high in carbon content and low cost, it can be effectively used in various applications such as soil amendment, fuel and water [12, 13]. Many researchers have realised that the porosity and functional group present in biochar are the most favourable properties for a wide range of applications. However, biochar applications in various fields have been restricted due to unmodified biochar having very limited functionality, a relatively small surface area and poor pore properties [14]. For instance, raw biochar shows a lower ability to adsorb various organic and inorganic contaminants from highly [15, 16] concentrated waste water or polluted water.

Therefore, obtaining a class of biochar with a well-developed porosity, large surface area, an abundant availability of functional groups, high physiochemical stability, etc. would be most beneficial. As a result, there has been growing attentiveness among the scientific community to activate biochar as a key material in accelerating research for better environmental applications [17–19]. Biochar-derived activated biochar has been paid increasing attention due to the implementation of two main activation techniques discussed in a later section, the physical and chemical activation for improvement of physical and chemical properties [20]. The resulting biochar after activation is noted for its improvement in quality. Thus, activated biochar is likely to be used in an extensive array of applications regarding the environment. Activated biochar has already been used in soil remediation, most probably for removal of organic pollutants and heavy metals in soil via absorption [21]. Many studies have already shown that activated biochar plays a significant role in the removal of organic pollutants (especially antibiotics), inorganic pollutants and heavy metals from water and wastewater [22]. In addition, according to Zhang et al. [23], activated biochar is becoming more active in the esterification process, which decreases fatty acid content and increases catalytic activity in biodiesel production. Nowadays, researchers are paying extensive attention to activated biochar electrodes, due to their well-improved surface area and porous structure, for further application as supercapacitors for energy storage [24, 25]. In addition, activated biochar is considered the ideal electrode material when compared to granular activated carbon, graphene, graphite granule and carbon nanotubes [26]. Activated biochar is also used as fuel in direct carbon fuel cells which leads to maximum power density [27].

1.2 Biomass feedstock for activated biochar preparation

The lignocellulosic biomass is a form of agricultural sector waste and forest waste, which are abundantly available. The lignocellulosic biomass is composed of carbohydrate polymers, such as cellulose and hemicelluloses and aromatic polymer mainly known as lignin as shown in Fig. 1 [28]. The efficient conversion of lignocellulosic biomass into biochar through different thermochemical conversion routes, followed by the preparation of activated biochar using an activation process, is an important approach in the environmental pollution control strategy. The components of biomass such as cellulose, hemicelluloses and lignin provide a rigid structure to the plant because they are strongly intertwined and chemically bonded using non-covalent forces. Biochar-derived activated carbon has a well-developed surface area containing internal porous structure along with a broad spectrum of functional groups. Therefore, it is crucial to select precursors to achieve adsorption properties, textural features and micro-nano structure and enhance the applicability of activated biochar.
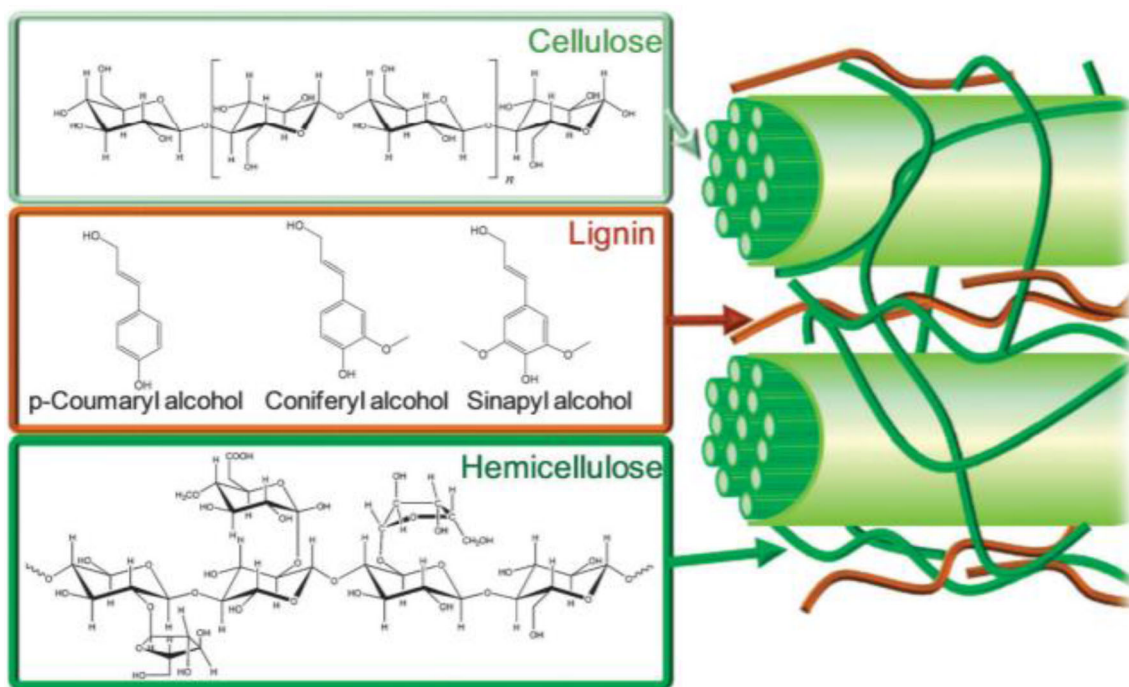
Fig. 1 Structural composition of lignocellulosic biomass [28]

In this sense, as per various scientific literatures, utilising lignocellulosic resources to prepare low-cost activated biochar has had significant benefits in recent years, due to its role in minimising the cost of agro-waste disposal as well as the negative effect on the environment [29]. The precursor material for the development of low-cost activated biochar should be abundant, diverse, renewable, non-hazardous to the environment and available at a minimum price. As we mentioned earlier, to obtain the desired surface, textural and structural properties of activated biochar, lignocellulosic biomass should have a higher percentage of fixed carbon along with minimum ash content [30]. Many efficient and interesting sources are available, such as woody biomass, herbaceous, agricultural waste or industrial biomass waste. Among these, different parts of crops, including shell, stem fibres, seed, husk and stones, among others, are the main aspects that have to be considered in the selection of precursors for the development of low-cost activated biochar.

A profound comprehension of the physical and chemical properties of lignocellulosic biomass would help in designing and further operations related to biomass conversion processes. The physicochemical properties of biomass for the production of activated biochar are based on its particle size, density, grindability, thermal properties, proximate properties, elemental composition etc. The main elemental composition of lignocellulosic biomass consists of carbon, hydrogen, oxygen, nitrogen, calcium and potassium, and small concentrations of Si, Al, Mg, Fe, P, Cl etc. Lignocellulosic biomass is currently not regarded as a direct energy conversion source due to

its seasonal variation, high moisture content, volatile nature, low bulk density and the wide diversity in its physicochemical composition. To address these limitations, there is a need for pre-treatment of the biomass followed by a conversion process. Nonetheless, the most significant benefit of utilising renewable lignocellulosic biomass lies in the possibility of generating functional materials such as fertiliser [31], catalysts [32], electrodes [33], liming and neutralising agents [34] and adsorbents for air and water treatment [35]. The physicochemical characterisation of some lignocellulosic residues used for the preparation of activated biochar is depicted in Table 1.

2 Production process for activated biochar

The preparation of activated biochar from lignocellulosic biomass is carried out in two main steps. The first step in the production of activated biochar is achieved through carbonisation or pyrolysis of raw materials [51]. Throughout the process of carbonisation, thermochemical reactions take place and moisture content, as well as volatile matter, is released from the biomass. From the produced char or biochar, activated biochar can be prepared by using three different experimental processes, including physical, chemical and combined physical and chemical activation. In addition, simple thermal activation in the presence of nitrogen atmosphere [52] as well as microwave radiation [53] methods indicates good techniques for activated biochar production.

Table 1 Characteristics of some lignocellulosic residues used as precursor for activated biochar preparation

Precursor	Proximate analysis (% w/w)				Ultimate analysis (% w/w)				Lignocellulosic composition (%)			Reference
	Moisture	Volatile	Ash	Fixed carbon	C	H	N	O	Cellulose	Hemicellulose	Lignin	
Peanut shell	–	–	–	–	41.53	5.55	2.12	–	45.30	8.10	32.80	[36]
Coconut shell	5.62	71.4	1.11	23.3	48.7	6.34	1.52	43.4	–	–	–	[37]
Wheat straw	6.30	66.96	5.97	20.77	42.66	5.48	0	39.59	33	20	15	[38]
Palm shell	5.50	70.00	4.28	23	47.77	5.98	0.90	45.31	–	–	–	[39]
Rice straw	18	55–65	15–20	12–22	48–51	6–6.2	< 0.2	36–43	38	32	12	[40]
Orange peel	9.2	76.5	3.1	20.4	46.63	6.04	0.23	47.05	n.a.	n.a.	n.a.	[41]
Grape stalk	7	63.1	8.7	21.2	41.58	4.92	1.18	52.16				[42]
Tomato stems	3.58		10.6						27.03	21.1	16.01	[43]
Peach stone	9.3	71.7	1.1	17.9	45.92	6.09	0.58	47.38	46	14	33	[44]
Guava seed	6.5	28.8	0.3	65.2					28	15.5	41.7	[45]
Almond shell	10.2	81.2	0.70	7.9	49.50	6.30	0.2	43.97	24.5	33.2	25.2	[46]
Sago palm bark	9		2.9		45.16	6.30	0.014	48.54				[47]
Date pits	10.3		1.30		45.63	7.11	0.72	46.47				[47]
Barley straw	9	77.2	5	17.3	45.4	6.1	0.7	41.92	38	35	16	[48]
Palm kernel shell		77.4	2.5	20.1	43.6	4.9	0.5	51.6	30	21.4	47.3	[49]
Tomato waste	2.95	82.67	1.58	12.80	58.95	8.21		29.77	33.17	23.79	34.50	[50]

2.1 Carbonisation/pyrolysis process

Carbonisation, or pyrolysis of lignocellulosic biomass, is sometimes carried out prior to the activation process, a process during which raw material undergoes thermal decomposition to enrich the carbon content in biochar [54, 55]. The carbonisation or pyrolysis of raw material/precursor takes place at a temperature usually ranging between 400 and 850 °C in the absence of oxygen [56]. In this process, different factors were taken into consideration such as the rate of heating, inert atmosphere and residence time [57, 58]. This creates a significant effect on the carbonisation process. During the carbonisation, cellulose, hemicelluloses and lignin undergo thermal decomposition reactions such as depolymerisation, crosslinking and fragmentation at a specific temperature, resulting in solid, liquid and gaseous end products. The solid and liquid end products from the carbonisation process are referred to as "biochar" and "biooil," whereas the gaseous product is referred to as syngases, which is a mixture of carbon monoxide, carbon dioxide, hydrogen and hydrocarbons.

Normally, biochar obtained at a high carbonisation temperature (600–700 °C) seems to be highly aromatic in nature with an advanced carbon layer. However, the availability of functional groups (particularly H and O) is very less in the resulting biochar, due to the deoxygenation and dehydration of precursor material which normally takes place at high temperature [21, 59], and therefore biochar also showed a low ion exchange capacity [4], while the biochar which produced low carbonisation temperature, usually between 300 and 400 °C, shows highly diversified organic characters, such as the availability of cellulose and aliphatic type components, as well as the abundance of functional groups (C=O, C, H, etc.) on the surface of biochar [60, 61].

The primary end product from the carbonisation process, biochar, shows some initial porosity, but it cannot be used in industrial applications because porosity is too low. The pores formed in the carbonisation process are filled with tar [58], so secondary processes are necessary to generate a highly developed, activated biochar. As the carbonisation temperature increases above 700 °C, the produced biochar showed a positive relationship with fixed carbon (carbon stability); pH; ash content; surface area; electrical conductivity; the total content of N, P, K, C, Ca and Mg; and microporous structure, while having a negative relationship with biochar yield, volatile matter, the total content of H and O, average pore size, the density of functional groups and the ratio of H/C, O/C, (O + N)/C and (O + N + S)/C respectively [62, 63]. Moreover, the biochar produced at high temperatures shows better quality but yields less. Indeed, decreases in biochar yield at higher temperatures could be due to either further primary decomposition of raw materials at high temperature or secondary decomposition of char residue providing a maximum yield of non-condensable gases [64].

2.2 Biochar activation

The main purpose of the activation process is to enhance the surface area, pore volume and pore diameter, and increase the porosity of the resultant-activated biochar or carbon. Physical and chemical activation are the most commonly used

processes for the preparation of activated biochar [20]. Both treatments influence the physical properties, like the shapes and sizes of the resultant product [65]. Physical activation is also known as thermal or dry activation [66]. In the physical activation process, the precursor will be pyrolysed or carbonised (< 800 °C) and then activated using steam or CO_2 [58]. It means that there are two main steps in physical activation: carbonisation and activation step. Physical modification mainly composed of steam and gas purging. Conversely, in chemical activation (also known as wet oxidation) [67], precursors or biochars are impregnated by chemical activating agents and then heated in a furnace at a desired operating temperature under inert conditions [68, 69]. The process is comprised of the following steps: acid modification, oxidising agent modification, alkalinity modification, and metal salt and carbonaceous material modification. Chemical activation or modification is more widely used than physical modification because of its some distinctive salient features such as the following: (1) requires low process time and activation temperature; (2) activated biochars possess larger surface area (3600 m^2/g); (3) better activated biochar yield; (4) well-developed and distributed microporous structure. The chemically activated biochar with well-developed microporous structure and the larger surface area plays a vital role for extensive environmental applications [70–72]. The detailed classification of biochar activation process and further its possible effects are shown in Fig. 2.

2.2.1 Physical activation

In the physical activation process, the biochar sample was activated at a high temperature of up to 900 °C over a 60-min interim of repose under steam while partial pressure was held at up to 53 kPa, respectively [73]. Biochar pores are formed in the steam activation process; it might be due to the reaction with steam that results in conversion of the volatile matter and fixed carbon into carbon monoxide and carbon dioxide. The main purpose of steam modification of biochar is to increase the surface area, pore volume and surface morphology by decreasing the aromaticity, as well as the polarity. The resultant increase in the surface area of steam-modified biochar is due to the corrosion of the activated biochar surface and the emission of additional syngases, mostly in the form of hydrogen [74]. Moreover, steam modification removes the trapped particles or volatile gases and thereby causes the enhancement of pore volume, as well as the development of internal pores on the modified biochar surface.

To optimise these properties, different modification times and temperatures are applied for the activation process to occur. However, steam-modified biochar provides a smaller surface area as compared to an acid or alkaline modification. Nonetheless, many researchers have widely adopted the steam modification process to improve the textural properties of biochar. Owing to this, Rajapaksha et al. [75] and Chakraborty et al. [76] carried out steam modification to improve the
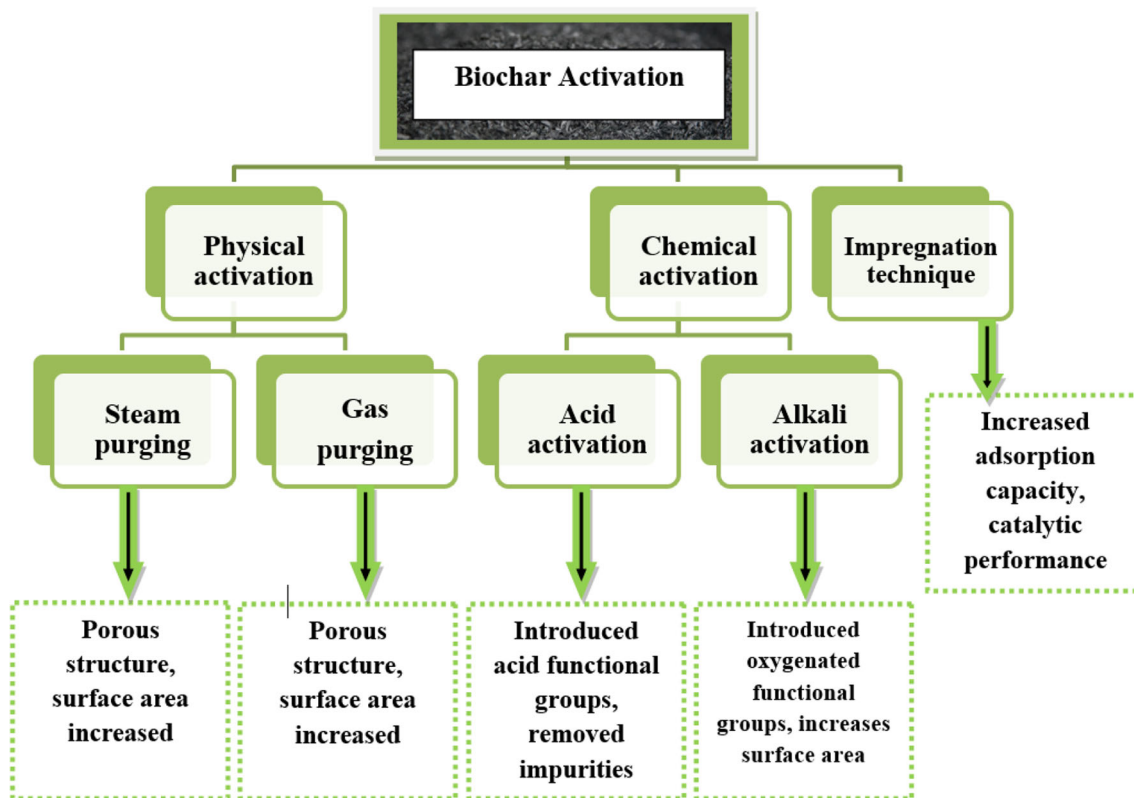

Fig. 2 Classification of biochar activation

textural properties of *Sicyos angulatus* L. invasive plant and aegle shell–based biochar from 4.40 to 308 m^2/g and 2.31 to 7.10 m^2/g, respectively. Furthermore, Sewu et al. [77] reported that steam-activated biochar showed superior textural properties, and the resulting biochar could serve as a promising viable adsorbent for waste water treatment. Furthermore, the steam-modified biochar contains a lower O/C molar ratio due to prepared biochar being hydrophilic in nature [78]. For example, due to lower H/C, N/C and O/C molar ratios in steam-modified biochar, it is rendered ill-suited for enhancement in surface functionality as compared to acid- and alkali-modified biochar, although the sorption capacity of modified biochar may be greater due to a higher micropore volume of the resulting modified biochar. Recently, Abu Bakar [79] produced biochar via steam modification from empty fruit bunch (EFB) at a pyrolysis temperature of 400–500 °C followed by steam modification and resulting biochar showed highest value of electrical conductivity (EC) which was 10.35 mS cm^{-1}. Bardestani and Kaliaguine [73] observed that steam modification increases the BET surface area of biochar from 50 to 1025 m^2/g, respectively. Marin et al. [80] prepared activated biochar from cherry stones by keeping the activation temperature between 350 and 500 °C using air as an activating agent. Air activation results in biochar with larger surface area, homogeneous microporosity and accumulation of quinine type functional groups. The air-activated biochar exhibits a well-developed porous texture that is extremely functional for the removal of non-polar or non-charged organic pollutants in solution [81], although the physical activation using oxygen or air is not recommended in the most of the cases because the reaction takes place very fast and due to this the carbonaceous material burns off in an irrepressible manner. The uncontrolled burning of the material leads to the random development surface area and porosity of material along with the formation of a large amount of surface oxide [82].

Gas purging (CO_2 modification) may enhance the surface area and pore volume of biochar and also build up the activated sites on the surface of biochar [83]. Shao et al. [83] observed a dramatic increase in surface area, micropore area and micropore capacity of activated biochar derived from corncob feedstock in a CO_2 atmosphere; after CO_2 modification, it was increased from 56.91 to 755.34 m^2/g. In case of CO_2 activation, carbon dioxide reacts with the carbon of biochar to form carbon monoxide (i.e. hot corrosion), thereby forming a microporous structure. Therefore, at ambient temperature, the gas sorption capacity of CO_2-modified biochar was much higher than that of unmodified biochar [84]. Pallares et al. [48] observed that under optimised conditions, the BET surface area and micropore volume of biochar modified by CO_2 activation were more than steam modification. In the experimental investigation, authors prepared activated biochar from barley straw using physical activation. They did this by taking two different modifying agents: pure steam and carbon dioxide. Optimal conditions for modifications significantly affect the surface area and micropore volume of modified biochar. Here, the authors analysed the most appropriate optimal conditions for carbon dioxide activation (at a temperature of 800 °C and hold time of 1 h). The authors then analysed the case of pure steam activation at 700 °C by keeping the same hold time. In addition to this, as temperature and hold time were increased, microporosity dramatically decreased while mesoporosity of resulting biochar increased. However, CO_2 modification aids the building of microporous structure because when carbon dioxide reacts with carbon of the biochar, it produces carbon monoxide, i.e., hot corrosion. Zhang et al. [85] performed combined modification of carbon dioxide and ammonia on biochar derived from soybean straw. The carbon dioxide-ammonia modification gives dual benefits: CO_2 modification assists in increasing surface area up to 627.15 m^2/g, while ammonification process assists in a building up the nitrogen functional groups on biochar surface which improves the adsorption capacity.

2.2.2 Chemical activation

Chemical activation is the most widely adopted process for activation. The chemical modification includes both one-step and two-step activation processes. During the one-step modification process, carbonisation and activation of biomass are achieved simultaneously using a chemical agent, while in the case of two-step modification process, carbonisation of raw material was followed by chemical activation of resulting carbonised end product in the presence of chemical agents or sometimes pre-treatment of biomass by mixing with chemical agents before carbonisation process. Chemical modification mostly includes acid modification, alkaline modification, metal salts or oxidising agent modification, and oxidising agent modification [86] etc. Table 2 compares the activation effect of several chemical activation methods.

Acid activation is necessary to modulate the physicochemical properties of biochar by introducing acid functional groups on the biochar surface for further application. The main reason for acidic modification of biochar is to eliminate the metallic impurities, in which the acidic functional groups largely alter the physicochemical properties of biochar. Commonly adopted acidic agents include sulphuric acid, hydrochloric acid, nitric acid, oxalic acid, phosphorous acid and citric acid [94]. As biochar modification agents, sulphuric and oxalic acids have shown to increase the sulfamethazine retention and maintain the pH of soil, thus proving to be a suitable method for soil amendment [5]. In addition, Ippolito et al. [95] found that acid-modified biochar also significantly influenced the calcareous characteristics of soil. By increasing the application rate of acidic biochar, soil nutrients, such as Zn, Mn and P, and soil organic carbon content increased; subsequently, soil pH dropped between 0.2 and 0.4. Acid

Table 2 Comparison of activation effects caused due to several chemical activation methods

Raw material	Chemical agent	Activation temperature	Activation effect	References
Forest waste	H_3PO_4, NaOH	600 °C	(1) More surface area (300–422 m^2/g) and pore volume (0.04–0.06 cm^3/g) for H_3PO_4-treated biochar, while lower for NaOH-activated biochar.	[87]
			(2) Highest drug and Cd removal efficiency for 5 M H_3PO_4-activated biochar (263.8 mg/g) than 1 M NaOH-based biochar (79.30 mg/g) respectively.	
Pine wood	K_2CO_3	250 °C	(1) Dye removal capacity 186.9 mg/g.	[88]
			(2) Possessed medium surface area (95.6 m^2/g) and pore volume (0.18 cm^3/g) of biochar.	
Sorghum distillers grains	NaOH, KOH	500–800 °C	(1) KOH-activated biochar have highest ammonium nitrogen removal capacity than NaOH-activated biochar.	[89]
			(2) KOH-treated biochar contains higher functional groups.	
			(3) Although NaOH-modified biochar had larger surface area (132.8 m^2/g) than KOH-treated biochar (117.7 m^2/g) respectively.	
Wood residues	KOH	900 °C	(1) KOH-modified biochar is highly microporous and more availability of surface functional groups.	[90]
			(2) Minimum Cu^{2+} adsorption capacity as compared to CO_2-activated biochar.	
Poplar chips	$AlCl_3$	550 °C	(1) The carbon content in $AlCl_3$-modified biochar is significantly reduced as compared to pristine biochar.	[91]
			(2) Surface area has been increased due to Al activation.	
			(3) The adsorption capacity for NO_3^- and PO_4^{3-} has been significantly improved.	
Wheat straw	HNO_3	90 °C	(1) Activated biochar showed higher content of COO groups.	[92]
			(2) Better U(VI) adsorption capacity 40 times more than pristine biochar.	
Rice husk	H_2SO_4 and KOH	450–500 °C	(1) Larger surface area than raw biochar.	[93]
			(2) Excellent adsorption performance for removal of tetracycline from aqueous solution (58.8 mg/g).	

modification have also been found to improve the surface area of resulting biochar, while the impregnation ratio, type of acids and activation temperature were found to increase the surface area and mesopore volume of biochar. For example, Peng et al. [96] found that the surface area of biochar obtained from reed increased from 58.75 to 88.35 m^2/g after activation with 1 M hydrochloric acid. However, as the activation temperature (600 °C) and impregnation ratio (2) increased, the maximum BET surface area of 1547 M^2/g was displayed by starch rice food waste derived from phosphoric acid–modified biochar [97].

Acid modification of lignocellulosic biomass using phosphoric acid may enhance the thermal stability of the resulting biochar and the synthesis of surface acidity on biochar surface through the availability of oxygen-phosphorous surface groups [98]. Such phosphoric acid–modified biochar is used as a catalyst in hydrocracking reaction for obtaining tire pyrolysis oil [99] and also acts as an acid catalyst in alcohol dehydration reaction [100]. The surface area and functional groups present on the biochar surface significantly affect the adsorption capacity of modified biochar. The phosphoric acid–derived modified biochar, having large surface area

and availability of more oxygen-containing functional groups, therefore, results in biochar having higher affinity towards the adsorption of Cu(II) and Cd(II) heavy metal ions as compared to pristine biochar [101]. Iriarte-Velasco et al. [102] prepared porous modified biochar by acid activation (H_2SO_4 and H_3PO_4) on pork bones. The microporosity of the resulting sulphuric acid–activated biochar was enhanced up to 263%, at higher impregnation ratio. In addition, acid modified at impregnation ratio 0.2 $mmol_{acid}/g_{precursor}$ increased the surface area of modified biochar by about 80%, compared to untreated bone char. On the contrary, weak acids such as citric acid and oxalic acids can also build up the carboxyl functional group on the biochar surface, but after modification, Lei et al. [103] observed that the surface area of biochar slightly decreased from 1.57 to 0.69 m^2/g and 1.21 m^2/g, respectively. As per various literatures, the acid-modified biochar has a lesser surface area as compared to other activation processes, which may be due to the destruction of pore structure. However, oxygen content on acid-modified biochar was significantly increased as compared to other modification processes. At present, different preparation conditions are available, which can vary according to feedstock, activation temperature, impregnation ratio, types of acids etc.

The alkaline activation of biochar is carried out to enhance the surface area and oxygen-containing functional groups on the resulting modified biochar. The most commonly used alkali-activating agents include sodium hydroxide and potassium hydroxide. The biochar produced from carbonisation process was soaked in alkaline agents in different concentrations at room temperature 20–22 °C. The soaking and stirring can take as long as 6–24 h, depending on the type of precursor material used for alkaline activation. After the washing and drying of biochar, it is further pyrolysed in a reactor within a 300 to 700 °C temperature, under nitrogen environment for 1–2 h. This will help obtain the resulting functionalised modified biochar [6]. In alkaline modification, a positive surface charge is created on biochar surface which in turn helps in adsorption of negatively charged contaminants. The KOH-modified biochar is considered environmentally friendly, a cost-effective adsorbent material for the removal of heavy metals present in waste water. Due to alkaline modification, KOH-modified hydrochar showed that increases in oxygen-containing functional groups and aromatic and carboxyl groups result in increases in cadmium adsorption capacity (30.40–40.78 mg/g) which was 2–3 times more than the unmodified hydrochar (13.92–14.52 mg/g) [104]. KOH-modified hydrochar possesses less apparent BET surface area (0.4–1.8 m^2/g) and pore volume (0.002–0.006 cm^3/g), when compared to unmodified hydrochar (4.4–9.1 m^2/g) respectively. In addition, KOH modification was found to increase the surface area (18.69 m^2/g) and pore volume (0.040 cm^3/g) of the eucalyptus sawdust-derived biochar, which is prepared by hydrothermal carbonisation, and used for the removal of hexavalent

chromium [105]. However, Sun et al. [104] observed that wheat straw–derived KOH-modified biochar, through hydrothermal carbonisation, showed a decrease in surface area (from 4.4 to 0.69 m^2/g) respectively. The authors conclude that the decreases in surface area may be related to availability of organic compounds in derived biochar, causing pore blockage, which were not converted into liquid phase during KOH activation [30].

In addition, the type of precursor feedstock, preparation method and operating conditions during alkaline modification can severally affect the surface area and pore volume of the biochar. Cazetta et al. [106] reported that an alkaline agent like sodium hydroxide is less corrosive and more economically feasible compared to potassium hydroxide. The sodium hydroxide–activated biochar was showed to be an effective material for adsorption of Cd_{2+} (0.648 mg g^{-1}), Pb_{2+} (44.64 mg g^{-1}) and Ni_{2+} (6.20 mg g^{-1}); however, the adsorption capacity exhibited by NaOH biochar was more than other acid-activated biochar [107]. Hu et al. [108] found that sodium hydroxide–modified biochar possesses a lower surface area (6.88 m^2/g) and pore volume (0.0052 cm^3/g) than sulphuric acid–modified biochar (163.57 m^2/g) and pore volume (0.0728 cm^3/g), resulting in low nitrate removal capacity. The reduction in surface area and pore volume of NaOH-modified biochar may be due to sodium carbonate crystal formation and some precipitate on the surface of the biochar causing a decrease in the adsorption capacity. As the pyrolysis temperature increased, the surface area followed by pore volume and pore size also significantly improved, reported by Hasnan et al. [109]. The authors carried out pyrolysis of tapioca skin at 600 °C followed by activation using sodium hydroxide reagent resulting in a maximum surface area up to 78 m^2/g respectively.

However, type of feedstock, types of alkali reagents and impregnation ratio may significantly affect physicochemical properties of biochar. Owing to this, Shen and Zhang [110] observed that impregnation ratio of KOH and biochar most notably affects the physical properties of resulting biochar. When mass ratio was 3, highly functionalised modified biochar was obtained. Therefore, the effect of alkaline modification on biochar is influenced by precursor material and preparation procedure. Trakal et al. [111] reported that alkaline modification assist to improve both physical and chemical properties of the modified biochar; further authors also realised that 2 M KOH-activated brewers draft biochar showed maximum pore volume due to changes in pore distribution, but BET surface area remained the same for both biochar samples before and after alkaline modification.

Impregnation of biochar helps to improve the physicochemical properties of resulting biochar by forming composites, which may increase the mass yield as well as the sorption behaviour of modified biochar. Impregnation of biochar using metal oxides or salts can improve the characteristics in terms

of adsorption, magnetism and catalysis. Recently, there has been some interesting biomass-derived modified biochar impregnated with metal oxides including MnO, ZnO, CaO, FeO etc. and metal salts like $AlCl_3$, $LaCl_3$, $MgCl_2$, $FeCl_3$ etc. have been activated to achieve the goal of enhancing the adsorption capacity for negative ions [112]. Therefore, it is necessary to prepare a metal oxide– or salt-based functionalised modified biochar for efficient removal of anionic pollutants. Zinc oxide–impregnated sawdust biochar showed maximum apparent surface area of 518.54 m^2/g, larger pore size and newly generated hydroxyl groups, which showed good performance for both removal of p-nitrophenol and Pb(II) from wastewater [113]. Recently, Liang et al. [114] introduced newly synthesised modified pine biochar by impregnation of magnetic ferromanganese oxide which showed maximum BET surface area of 666.22 m^2/g, pore volume of 0.22 cm^3/g and average adsorption aperture of 2.43 nm, which was much higher than pristine biochar having 13.08 m^2/g, 0.01 cm^3/g, and 1.32 nm respectively. Due to significant characteristics, modified biochar showed improved adsorption capacity (100.74 mg/g) of tetracycline hydrochloride from wastewater, which was much more compared to biochar (33.76 mg/g). Further, the authors also observed that the best adsorption performance was attained at pH 4. Consequently, the initial pH of the solution significantly affects the surface charge, molecular structure of heavy material, active sites of modified biochar and ion state of surface functional groups which influences the adsorption performance as a result [115]. Akgül et al. [116] prepared modified biochar from industrial tea waste by synthesising metal salts including Mg, Fe, Mn and Al, which were performed for PO_4^{3-} and Cd^{2+} sorption. Metal salt–impregnated biochar composites are rich in functional groups; especially Mg–synthesised biochar showed best sorption capacity of PO_4^{3-} and sorbing up to 30% at 20 mg PO_4^{3-} l^{-1}. Metal salt–impregnated biochar efficiently removed heavy metals due to the availability of hydroxide function group on the surface of each metal.

3 Physicochemical properties and analytical techniques of activated biochar

The physicochemical properties of biochar primarily depend on the types of raw material used and preparation conditions (for example reactor type, temperature, residence time, etc.), while on the other side, the physicochemical properties of activated biochar, such as surface area, pH, molar ratios (H/C, O/C, N/C), surface charge, mineral content, elementary compositions and binding sites, vary according to modification methodology. In addition to reactor type, Wang et al. [117] used a fluidised bed reactor for the preparation of corn stalk–derived activated biochar. The fluidised bed reactor plays a crucial role by developing the structure and

morphology of produced activated biochar. The physically activated biochar exhibits the microporous structure and enhanced surface area up to 880 m^2/g, while chemically activated biochar using H_3PO_4 showed mesoporous structure and have a surface area up to 600 m^2/g respectively. Niksiar and Nasernejad [118] found that spouted bed reactor is a more suitable equipment for the activation process as compared to fluidised and fixed bed reactor. Spouted bed promotes excellent mixing of material and well distribution of heat inside the reactor. Physically activated pistachio shell biochar in spouted bed reactor showed higher BET number, i.e. surface area of 2596 m^2/g with a burn off about 90% at activation temperature 850 °C for 20 min of activation time. The reason for the higher BET number is the minor heat and mass transfer resistances took place inside the spouted bed reactor. In addition, steam activation of biochar in vacuum pyrolysis reactor showed efficient process for the preparation of meso- and macroporous-activated biochar. The biochars obtained at 800 °C/steam have a larger surface area of 570 m^2/g, micropore volume (0.157 cm^3/g), C (78 wt%), N (0.9 wt%) and H (0.6 wt%), respectively [119]. However, steam-activated biochars obtained through vacuum pyrolysis reactor possess minimum concentration of functional groups, while the surface area has extensively increased from 50 to 1025 m^2/g respectively. Steam activation increased ash and fixed carbon content in modified biochar [73]. The heating rate of vacuum pyrolysis is distinguished from that of slow pyrolysis due to vacuum condition inside the reactor; it is to be characterised by quick removal of pyrolytic gases within a short residence time. Therefore, due to the rapid removal of syngases, the primary pyrolysis process significantly minimised secondary char formation and cracking reaction [120]. This plays an important role in its prospective energy and environment application, especially in contaminant removal. In addition, after the biochar activation, it is crucial to analyse the characteristics of biochar in terms of its morphology and chemical composition. There are several analytical techniques used for this process, such as nitrogen adsorption isotherm, Raman spectroscopy, NMR, NEXAFS technique, Fourier transform infrared spectrometry (FTIR), X-ray diffraction (XRD), scanning electron microscopy (SEM), transmission electron microscopy (TEM), X-ray photoelectron spectroscopy (XPS) technique, Boehm titration process, Barrett-Joyner-Halenda (BJH) methodology and X-ray spectroscopy (EDS), to name a few, all of which were briefly summarised.

The nitrogen adsorption isotherm is mostly used to determine the surface area of biochar at different partial pressures of N_2. Specifically, Raman spectroscopy is a reliable method used to determine the carbon structure as well as structural disorder and defects in the biochar sample. This is a scattering method, which utilises an incident laser to generate a vibrational response in the char being studied [121]. NMR is also a valuable and nondestructive technique utilised to investigate the structural

composition of activated biochar. The degree of aromaticity in the biochar matrix is a significant feature in the char structure, which can be determined by using NMR technique [121].

Near-edge X-ray absorption fine structure spectroscopy (NEXAFS) is a prominent functional tool for the chemical characterisation of activated biochar. It is a synchrotron-based process that mainly uses the intense, tunable and polarised X-ray beams to examine the electronic states of the selected sample. Electron spin resonance (ESR) and electron paramagnetic resonance (EPR) are the spectroscopic tools that can be used to identify the species with unpaired electrons [122].

FTIR peaks are typically used to identify the difference of functional groups present on biochar surface. The peaks at different positions in the spectrometry indicate the availability of different functional groups: a peak about 3400 cm^{-1} typically represents the availability of –OH groups; at about 1600 cm^{-1} indicates stretching of C=O; at about 1260 cm^{-1} means availability of carboxylate –COO– groups; at around 1050 cm^{-1} shows the availability of carboxylic; at around 800 cm^{-1} represents the vibration of aromatic C–H; and at 540 cm^{-1} gives an indication of –C–Br– [123].

XRD technique is used to measure the carbon crystallites by measuring the intensity and angle of diffracted beams. Most commonly, carbon crystallites are classified into two categories, graphitised and non-graphitised carbon. A sharp and narrow reflection pattern is recognised as graphitised carbon, while a broad reflection pattern indicates non-graphitised carbon [124]. The surface morphologies can be observed by using SEM analysis, which is typically based on the interaction between biochar samples and electron beams. As with SEM, the TEM analyser is also used to measure surface morphologies with a high resolution. Additionally, EDS can identify the molar fraction present in the chemical composition of a given biochar sample.

X-ray photoelectron spectroscopy (XPS) is used to investigate the surface groups present on the biochar. Besides, XPS technique plays a significant role to understand the changes that occurred in the biochar structure at different pyrolysis temperatures [125]. Boehm titration process is primarily used to determine the acidic and basic functional groups present on the activated biochar. Barrett-Joyner-Halenda (BJH) methodology is utilised to determine the pore volume and size of biochar [126]. Most preferable techniques were used for analysis of activated biochar which is presented in Fig. 3

3.1 Physically activated biochar

A steam-activation process has been widely adopted by many scientific communities to enhance the textural properties of biochar. Steam-activated biochar demonstrates a higher surface area, higher porosity and higher pore volume, but no significant effect on pore size. Most commonly, pore size remains largely unchanged [77]. CO_2 activation builds up a higher microporous structure than steam activation [48]. In addition, during the initial phase of activation, CO_2 activation favours increases in the microporosity of biochar, whereas in the case of steam activation, microporosity widening is evidenced. Steam-activated biochar contains less hydrogen, carbon and oxygen content on its surface, resulting in lower H/C, O/C and N/C molar ratios when compared to biochar or chemically activated biochar. The reduction in H/C and O/C ratios at elevated temperatures is attributable to the hydrophilic nature of biochar or the loss of OH groups due to dehydration reaction [48, 75], while greater aromaticity in steam-activated biochar may be attributable to hydrophilicity/stability [127]. In addition to the physical properties of biochar, some chemical properties of steam-activated biochar, such as polarity, hydrophobicity, cation exchange capacity, acidic or basic characters, are also analysed based upon the availability of functional groups on the surface of biochar. These properties can have a significant effect on the adsorption capacity of various pollutants. The concentration of mineral elements in steam-activated biochar is always lesser when compared to CO_2 and chemically activated biochar. Overall, steam-activated biochar is not favourable to improvements in surface functionality due to lower polarity (O/C, N/C ratio) and aromaticity (H/C) when compared to raw biochar, as well as activated biochar prepared from acid and alkali activation. Table 3 shows the physicochemical properties of physically activated biochar from different lignocellulosic biomasses.

3.2 Acid-activated biochar

Acid-activated biochar introduces a large change in physicochemical properties: delivering selectively larger surface area and more oxygen-containing functional groups on the biochar surface. Phosphoric acid–activated biochar from pine sawdust showed maximum specific surface area of 950 m^2/g [102]. Similarly, Vithanage et al. [5] observed more surface area and pore volume for bur cucumber biochar activated with oxalic and sulphuric acid. However, in some cases, it was pointed out that acid-modified biochar showed lower surface area than other activation processes, which was the result of the pore structure breaking down. Vaughn et al. [132] also observed decreases in surface area, micropore surface area, pH, electrical conductivity and cation exchange capacity of sulphuric and oxalic acid–activated biochar, as compared to untreated biochar. Acid activation after pyrolysis can reduce the pH of biochar; therefore, lower pH biochar has a significant potential for further application in alkaline calcareous soil [133]. Vaughn et al. [132] noticed slight increases in H/C and O/C ratio of sulphuric acid–activated *Paulownia elongate* biochar and oxalic acid–activated biochar as compared to untreated biochar, respectively. In addition, authors also remarked that average values of O/C, H/C and N/C molar ratios were found to be higher as compared to other activation

Fig. 3 Analytical techniques used for activated biochar characterisation
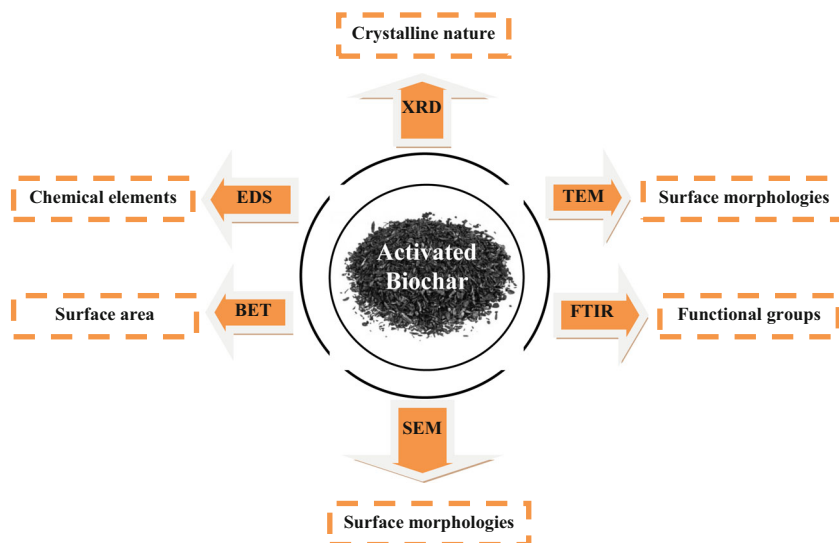
process owing to the low carbon content in the acid-activated biochar. However, the acid-activated biochar showed more oxygen and oxygenated functional groups on the surface of biochar than steam and chemical activation [134]. According to Vithanage et al. [5], when H/C and O/C ratios of biochar increased, it caused a reduction in hydrophobicity. Nitric acid–activated weed biochar showed lower carbon and hydrogen content, while nitrogen and oxygen content subsequently increased. This may have happened due to more intensive formation of aromatic compounds on biochar surfaces containing nitrogen in the presence of C and O functional groups on the biochar surface, and may be a result of the destruction of the pore structure in the biochar [135]. Further, authors also observed that as the concentration of nitric acid rises, there was a resulting increase in acidic functional groups on biochar surface such as phenol, carboxylic acid and lactone groups. In addition, as polarity increases, there is higher adsorption of organic and inorganic contaminants from the waste water. Recently, Zhang et al. [136] prepared activated biochar using three different chemicals, i.e. H_2O_2, HCl and NaOH, in order to efficiently remove nitrobenzene (NB) from the waste water. Acid-activated biochar (HCl BC) was found to be an effective remediation material for efficient removal of NB owing to the enhanced electron transfer rate, high surface area, increased acidic functional groups and negative surface charge on HCl-BC.

3.3 Alkali-activated biochar

Alkali activation ensured good physicochemical properties of biochar. According to El-Khateeb et al. [137], the KOH-activated biochar led to the maximum internal surface area, which may be fifty times more than the pristine biochar. Alkaline activation improved the cation exchange capacity, surface area and thermal stability; therefore, the resulting biochar exhibited more adsorption capacity than the original biochar. Alkaline activation generates higher internal surface area and the ability to alter surface functional groups compared to other engineering activation process such as acid and impregnation technique [138]. Further, Ding et al. [138] carried out alkaline activation (NaOH) using *Hickey BC* and observed that alkaline activation had significant effect on mineral composition of biochar. The calcium and magnesium contents were reduced while aluminium and potassium content were slightly increased after activation. Similarly, the carbon and nitrogen content in pristine biochar was found to be higher than that in activated BC, although a slight increase in atomic ratios (H/C and O/C) of activated BC (0.33 and 0.12) as compared to BC (0.26, 0.10) was observed. These results demonstrated that, due to alkaline activation, there was enrichment of hydrogen and oxygen functional groups on resulted BC sample; additionally, the depletion of carbon and nitrogen occurred, which led to the presence of hydrogen- and oxygen-containing functional groups on BC surface [59]. Sodium hydroxide activation may have multiple effects on the mineral structure of BC and therefore could concentrate or leach some minerals such as K (0.28–0.05), Ca (1.17–0.63), Mg (0.29–20) and Al (0.04–0.66). Similarly, KOH-activated BC from municipal solid waste exhibited increased surface area almost 69% than that of pristine BC and demonstrated positive AsV sorption capacity (25–31 mg^{-1}) [139]. According to Li et al. [140], availability of functional groups (amino, carboxylic and hydroxyl groups) played a significant role in metal sorption, but as activation temperature was increased, the availability of surface functional groups was reduced significantly. In addition, according to He et al. [141], KOH-modified BC had broadened properties like large surface area and porosity, and could provide a number of sites for iron particle loading. Table 4 shows the physicochemical properties for chemically activated biochar from different lignocellulosic biomass.

Table 3 Physicochemical properties for physically activated biochar obtained from different lignocellulosic residues

Precursor/particle size	Carbonisation condition	Activation agent	Activation condition	C (%)	H (%)	O (%)	N (%)	Molar H/C	Molar O/C	Molar (O + N/C)	Surface area (m²·g⁻¹)	Pore volume (cm³ g⁻¹)	Pore diameter (nm)	Porosity (%)	pH	References
Bur cucumber plants (< 1.0 mm)	700 °C/2 h, 7 °C/min	Steam	700 °C, 5 mL/min, 45 min	50.55	1.66	44.88	2.54	0.39	0.67	0.71	7.10	0.038	8.393			[75]
Giant *miscanthus* (4 cm)	N₂, 500 °C/1 h, 10 °C/min	Steam	800 °C	82.1	2.67	11.0	0.31	0.0325		0.138	322	n.a.	n.a.			[128]
Spent mushroom substrate	450 °C/4 h, 0.86 °C/min	Steam	800 °C/2 h, 2.0 mL/min	44	0.60	8.31	0.55	0.16	0.14		332	0.29	3.50	77.1	12.6	[77]
Bur cucumber plant	700 °C/2 h	Steam	700 °C/45 min, 5 mL/min	50.6	1.6	44.9	2.54	0.39	0.67		7.10	0.038	8.393			[129]
Tea waste	700 °C/2 h	Steam	700 °C/45 min, 5 mL/min	82.4	2.06	11.6	3.89	0.29	0.11		576.1	0.109	1.998			[129]
Bamboo waste (0.147 mm)	500 °C/2 h, 8 °C/min	Steam	500 °C/45 min, 5 mL/min	82.52	4.39	10.80	0.18	0.53	0.13	0.13	2.12	0.02	4.06			[130]
Corn cobs (0.2–0.6 mm)	N₂, 600 °C/1 h, 10 °C/min, 500 mL/min	CO₂	850 °C/1 h, 500 mL/min	91.4	7.14		1.46		0.08		755.34	0.3840 mL g⁻¹	2.02			[83]
Barley straw	N₂, 500 °C/1 h, 10 °C/min, 2500 cm³/min	CO₂	800 °C/1 h, 10 °C/min, 2500 cm³/min	51	0.5	10	1	0.114	0.149		789	0.3495	1.77			[48]
Barley malt bagasse (< 4 mm)	N₂, 800 °C/1 h, 10 °C/min, 0.25 mL/min	CO₂	900 °C/1 h, 10 °C/min, 0.15 L/min	68.32	1.46	28.38	1.74	0.21			80.5	0.0468				[131]

Table 4 Physicochemical properties for chemically activated biochar from different lignocellulosic waste

Precursor/particle size	Carbonisation condition	Activation agent	Activation condition	C (%)	H (%)	O (%)	N (%)	Molar H/C	Molar O/C	Molar (O+N)/C	Surface area (m²·g⁻¹)	Pore volume (cm³·g⁻¹)	Pore diameter (nm)	Porosity (%)	References
White wood	600 °C	KOH	875 °C/15 h, 3 K min⁻¹, 3.5:1 (KOH:Biochar)	64.55	2.23	23.03	0.13				2247	0.08	2.76		[142]
Corn straw	500 °C/1.5 h	KOH	800 °C/0.5 h, 2 g;500 ml (Biochar:KOH)	67.20	0.80	6.8	0.537	0.144	0.076	0.082	466.37	0.081	4.40		[14]
Sargassum waste	n.a.	KOH	800 °C/2 h, 2 (KOH:Biochar)								291.8	0.24	30.76		[143]
Corn cob	N₂, 400 °C/30 min	ZnCl₂	600 °C/2 h, 3:1 (Biochar:ZnCl₂)	84.76		7.24	3.11				1270	0.67	2.10		[144]
Sesame straw	600 °C/2 h, 5 °C/min	ZnCl₂	600 °C	74.1	1.8	21.1	2.7	0.29			319.4	0.2270			[145]
Tomato waste	n.a.	ZnCl₂	800 °C/1 h, 6:1 (ZnCl₂:TW), 10 °C/min	79.38	1.76	17.06	1.70				492	0.106	2.41		[50]
Pine wood sawdust (1–2 mm)	n.a.	H₃PO₄	600 °C/2 h, 10 °C/min, 2 ratio	80.2	2.4	16.7	0.7				1547	0.66	1.29		[97]
Pine sawdust (<1 mm)	650 °C/4 h	H₃PO₄	650 °C/2 h, 1:1 (acid:biochar)	63.0	2.26	27.1	0.29				900				[101]
Wheat straw	350 °C/30 min, 10 °C/min	H₃PO₄	350 °C/30 min, 10 °C/min, 2:1 (H₃PO₄:biochar)	68.23	2.17	25.50					471	0.45	11.25		[146]
Corn straw	n.a.	K₂CO₃	450 °C/2 h, 10 °C/min, 1:3 (CS:solution)	79.88	3.42	13.53	1.07	0.54	0.13	0.14	57.80		4.91		[147]
Pine chips	N₂, 300 °C/15 min	NaOH	800 °C/2 h, 10 °C/min, 3 g biochar:40 mL solution	72.6	0.77	21.3	0.65	0.127	0.221		1360	0.307			[148]

3.4 Metal oxide–activated biochar

Impregnation using metal oxide or salt helps to improve the physicochemical properties of BC by making new sites of composites, which usually enhances the sorption capacity. Metal oxide–derived BC always showed a stronger metal binding as compared to other activation processes. The H/C and O/C ratio in metal oxide–modified BC gradually decreased as activation temperatures increased, suggesting a strong decarboxylation and dehydration occurred during the activation process [149]. The H/C and O/C molar ratio usually decreased because of the incorporation of metal content from ZnO, CaO, MnOx and FeO composites on the BC surface, whereas an N/C molar ratio was always found to be greater in all types of activated BC samples. The metal oxide–modified BC showed more thermal stability than pristine BC, which might be due to the presence of thermally inactive minerals serving as diluents [150]. The surface roughness property of metal oxide–modified BC is always greater than simple BC, which might be because of minerals on the BC skeleton [149]. Metal oxide BC nanocomposites exhibited a larger surface area as compared to acid and alkali activation, which might be due to a surface effect [151]. As compared to other metal or salt oxides, manganese- and cerium nitrate–modified BC showed larger surface area, which can be attributed to the accumulation of minerals on the biochar surface [152]. Manganese oxide–modified BC contains a lesser percentage of carbon and other elemental components (Mn, k, Ca, Mg, Al and P) as compared to pristine BC. This is likely due to the dilution effect. In addition, Wang et al. [152] observed that MnOx–modified BC had double BET surface area and the pore volume increased almost seven times. This trend may be because of newly formed Mn-bearing minerals. The cation exchange capacity of Fe oxide–modified BC was always greater than acid- or alkali–activated BC. This may have been due to the presence of Fe oxide on the BC surface [153].

Thus, it was summarised that metal oxide BC had an ability to introduce higher surface functionalities than other (physical and chemical) activated BC. Such modified BC can usually be promoted as a reliable method for sorption of organic and inorganic contaminants from potable water and waste water. Table 5 shows the physicochemical properties for metal oxide–activated biochar from different lignocellulosic biomass.

3.5 Environmental applications of activated biochar

Activated biochar is efficient, cost-effective, economically feasible and environmentally friendly carbonaceous material. It has extensive environmental application prospects because of its distinctive features, such as high surface area, higher adsorption capacity, ion exchange capacity and microporosity. Environmental remediation becomes the primary

application of activated biochar. Therefore, recently activated biochar has gained significant attention due to its several environmental applications, e.g. soil remediation, water and wastewater treatment, as a catalyst, supercapacitors and fuel cell application as shown in Fig. 4.

3.5.1 Soil remediation

Activated biochar is considered a green remediation material for the adsorption of heavy metals and organic pollutants from the soil. The mechanism of activated biochar adsorption is mainly due to surface complexation, electrostatic attraction, hydrogen binding, pi-pi interactions and acid-base interactions.

Nontoxic sulphur-modified rice husk biochar showed increases in adsorption capacity of mercury (Hg^{2+}) in soil by ~ 73%, to 67.11 mg/g. The adsorption of mercury increase might be due to the forming of the low solubility of HgS and the availability of numerous active sites on the surface of sulphur-modified biochar [161]. Arsenic (As) is a potentially toxic and ubiquitous element that occurs in the surface of the soil. This has mainly occurred from lithogenic sources via weathering reactions, geochemical reactions and biological activities, which leads to environmental implications. Magnesium oxide–modified biochar is a very effective material for the adsorption and oxidation of arsenic. Because MgO–modified biochar possesses positively charged minerals across its surfaces, it can enhance the oxidation rate and allow more adsorption of As (V) [162]. In addition, Yu et al. [163] found that magnesium oxide–activated corn straw biochar has a great potential for the adsorption of arsenic present in red soil. The increased removal performance was attributed to the higher O/C ratio, lower H/C ratio, availability of oxygenated functional groups and higher surface hydrophilicity. The magnetite-activated water hyacinth biochar can potentially adsorb about 90% of As (V) [164], while the zinc oxide–modified rice straw biochar showed higher adsorption capacity of Zn^{2+} from the soil [165]. This discrepancy might be due to the selection of different feedstock and experimental conditions. In general, numerous factors such as pH, porosity, surface functional groups, surface charge, activation conditions and mineral composition can significantly affect the adsorption capacity of modified biochar, which has been discussed in previous studies [157]. The application of coconut shell–activated biochar with diluted hydrochloric acid and ultrasonication in soil remediation showed the effective removal of Ni, Cd and Zn by 57.2%, 30.1% and 12.7% respectively, in 5% addition of biochar. The good results of immobilising metals are due to the significantly improved microcosmic pore structure and surface functional groups [166]. Biochar modified with zero-valent iron improved adsorption of As and Cu, and which resulted in the maximum ecological recovery of bacterial communities present in soil

Table 5 Physicochemical properties for metal oxide–activated biochar from different lignocellulosic wastes

| Precursor/particle size	Carbonisation condition	Activation agent	Activation condition	C (%)	H (%)	O (%)	N (%)	Molar H/C	Molar O/C	Molar (O+N/ C)	Surface area (m² g⁻¹)	Pore volume (cm³ g⁻¹)	Pore diameter (nm)	Porosity (%)	pH	References
Millet bran (0.8 mm)	n.a.	MnOx	N₂, 600 °C/2 h, biomass:MnOx (1:10)								26.11	0.0139	5.558		10.58	[154]
Hickory chips	N.A.	KMnO₄	N₂, 600 °C/1 h, biomass: KMnO₄ (1:5)	66.10	1.49	–	0.03				205					[152]
Biomass	n.a.	MnO₂	–	17.48		45.38					161	0.020	2.54			[155]
Bamboo waste (10 × 5 × 2 mm)	n.a.	Mg	N₂, 500 °C/1 h,	25.7		26.4					377	0.54	5.77		7.80	[156]
Sugarcane residue	n.a.	MgO	N₂, 550 °C/1 h, 200 mL/min, 20% Mg biochar	27.17	2.37		1.47				40.6	0.372	22.38			[157]
Corn stover (0.18 mm)	n.a.	ZnO	N₂, 800 °C/1 h, 200 mL/min/20 min	63.00	1.06	10.47	1.07				448	0.454	4.05			[149]
Water hyacinth biomass	Argon, 700 °C/2 h, 3 °C/min	Zn(NO₃)₂	N₂, 380 °C/3 h, ZnO:BC (30%)								469.6	0.187	4.6			[158]
Peanut hull	n.a.	FeCl₃	N₂, 200 ml/min, 650 °C/1 h, 5 °C/min								145.25					[159]
Rape straw	n.a.	FeO	600 °C/1 h, 10 °C/min								6.82	0.0187	10.98			[160]
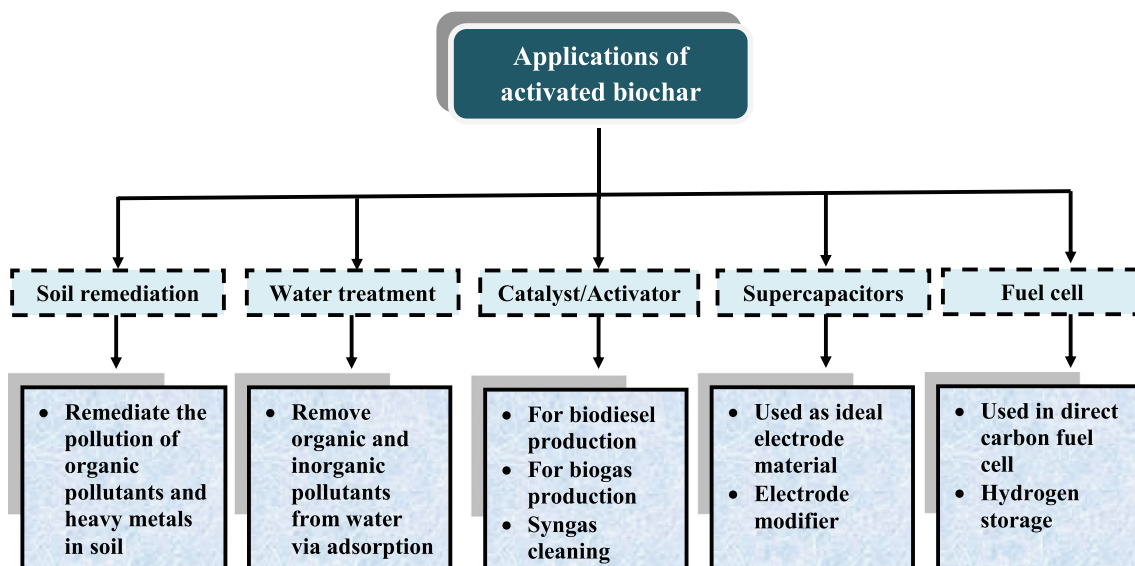
Fig. 4 Flow chart diagram of different applications of activated biochar

[167], which leads the assurance for in situ stabilisation of contaminated soil. However, the activated biochar not only adsorbs the heavy metals and organic pollutants but also neutralises the acid soil, and increases the soil fertility and cation exchange capacity. Moon et al. [168] observed that after 1-month treatment of oak and soybean stover–modified biochar in soil, the cation exchange capacity was improved with 5% biochar. The application of Fe–Mn corn straw–activated biochar could improve the soil redox potential, and activity of enzymes, and simultaneously reduce the As content in paddy soil [169]. In addition, activated biochar application in the soil can reduce the bulk density and significantly enhance the porosity, which may offer more availability of water. Therefore, the above results are indicating fine growth of roots, further improvement in crop growth and yields.

3.5.2 Water and waste water treatment

Many organic and inorganic contaminants and heavy metals present in water and waste water create a serious threat for both human beings and the environment. Many antibiotics are considered ubiquitous and toxic organic pollutants in the environment. Therefore, the promising and cost-effective material to remove the pollutants is urgently needed. Among all pollutants, heavy metals are very difficult for biodegradation, and conversion. Therefore, adsorption is the most reliable process in recent times. Activated biochar is cost-effective and a sustainable adsorbent carbonaceous material has recently paid significant research attention because of its wider applications in environmental prospects.

The adsorption of contaminants in water mainly attributed to the properties of targeted pollutants and the type of activated biochar. For example, the magnesium oxide modified biochar showed an increase in the removal rate of Pb^{2+} from 6.4

to 98.9%. The increase in removal rate was mainly attributed to the presence of biochar surface hydroxyl groups [150]. For Pb (II) sorption, manganese dioxide– and citric acid–activated biochar can remove 121.8 mg/g and 159.9 mg/g respectively [7, 170]. However, magnetic biochar synthesised by ZnS nanocrystal showed maximum adsorption capacity of 367.6 mg/g for Pb (II), which might be due to presence of zinc nano composite material along with magnetic biochar which made a reciprocal effect for the higher adsorption of Pb (II) [171]. Thus, it was observed the activation condition; the mainly activating agents had a remarkable effect on the physicochemical properties of activated biochar, which further impact on the adsorption capacity of modified biochar. The rice husk and municipal solid waste biochar activated with calcium (Ca^{2+}) and ferrous oxide (FeO) were shown 95% removal of As^{5+} and Cr^{6+} contaminations, which possibly occurred due to the electrostatic interaction and metal precipitation between activated adsorbent and heavy metals [172]. The haematite (γFe_2O_3)-modified biochar can also effectively remove the arsenic from drinking water; this happened due to the electrostatic interaction [112]. In addition, the coating of Fe^{3+} with biochar caused a significant change in the (O + N)/C ratios, O/C ratios and polarity indices [(O + N/C)], which influence the capacity of activated biochar for As^{5+} adsorption [173]. Thus, it was concluded that mineral compounds for activation processes such as magnetite, calcium oxide, haematite and manganese oxide have been extensively used to impregnate biochar because of its salient features such as a higher number of adsorption sites, magnetism and widespread distribution.

In addition to heavy metals, there are several organic contaminants that can cause serious threat when they enter in the living body via the food chain, water and air. For example, organic contaminants like phenol can affect the odour and

taste of drinking water. Therefore, activated biochar can adsorb these organic contaminants from aqueous solutions due to their adsorbing capacity and strong adsorbing affinity. For furfural removal, acid- or alkali-activated biochar showed good Langmuir adsorption capacities varying from 93.5 to 109 mg/g respectively. The increase in basic characteristics or basicity of alkaline-activated biochar and hydrophilicity of acidic biochar plays a significant role in the removal of furfural. In comparison, heat-treated bamboo-derived modified biochar showed the highest sorption capacity (253.2 mg/g) for furfural, because of hydrophobicity of modified biochar [174]. Citric acid–treated eucalyptus saw dust biochar showed sorption capacity of 158.6 mg/g for methylene blue removal, which might be possible due to the availability of carboxyl functional groups onto activated biochar [175]. Mostly, methylene blue showed increased adsorption capacity under the magnetic field. Also, as compared to acidic-, potassium permanganate– and hydrogen peroxide–modified biochar, the alkaline potassium hydroxide–treated biochar at pyrolysis temperature 550 °C showed higher phenol removal capacity (93.5 mg/g) from aqueous solution. In addition to alkaline characteristics of KOH-modified biochar, other factors such as pyrolysis temperature also influenced the adsorption capacity of modified biochar.

Similarly, activated biochars have shown a good adsorption capacity for the removal of various organic contaminants such as naphthalene, anionic dye, pentachlorophenol, 2,4,6-trichlorophenol and p-nitrotoluene [176–179]. Currently, some emerging organic pollutants such as pharmaceuticals (antibiotics), disrupting chemicals (EDCs) and personal care products are becoming one of the important environmental concerns because of their toxic interference to living organisms [180]. Biochars such as sulphuric acid–treated biochar, methanol-modified biochar and KOH-activated biochar are considered an effective material for the removal of antibiotics especially for tetracycline. Among these, the methanol-modified rice husk biochar showed enhanced adsorption capacity (95.6 g/g) for tetracycline as reported by Jing et al. [181].

3.5.3 Catalyst/activator

Presently, emerging applications of activated biochar are in refinery processes (syngas cleaning), air pollution control, biodiesel production, etc. [182]. Activated biochar has been used directly as a catalyst or catalyst carrier due to its outstanding features such as the availability of surface functional groups, surface area, porosity and chemical stability [183].

The biochar obtained from the heating of biomass possesses very limited surface functional groups, which restricts its use in the catalytic application. Therefore, several studies have been carried out for further modification of biochar, with the additions of activating agents during the pyrolysis process for improving the catalytic performance of activated biochar [184]. Firstly,

activated biochar as a catalyst plays an important role in transesterification; throughout the process, the glyceride present in vegetable oil reacts with alcohol having low molecular weight results in the formation of ester (known as biodiesel) and glycerol. The application of KOH-activated pomelo peel biochar as a catalyst in the transesterification process showed the highest biodiesel yield of 98%; the maximum yield was recorded because of the higher basicity of catalyst, which significantly improves the surface area and porosity of biochar [185]. The catalytic performance of activated biochar is mainly dependent on the structure, pre-treatment temperature and basicity of the catalyst. Similarly, CaO-modified rice straw biochar has shown a higher yield of biodiesel 93.4% during the transesterification process of vegetable oil with methanol. The maximum yield reached under certain conditions of activation temperature 700 °C and 30% CaO loading [186]. Secondly, the activated biochar can enhance the tar conversion during the gasification and pyrolysis process. Shen et al. [187] observed that during the pyrolysis process, decrease in tar yield and CO_2 concentration was mainly attributed to the application of Ni/Fe-modified rice husk biochar as a catalyst. Moreover, TGA analysis showed that biochar-supported catalyst has more thermal stability, and results in increasing the removal efficiency of heavy weight tar up to 92.3% respectively. Furthermore, as compared to other activating agents, Ni/Fe-based catalyst is also found cost-effective, extremely efficient and environmentally friendly for tar removal in biomass gasification and syngas conditioning [188]. The term biogas reforming is most efficiently used for the production of hydrogen, which is considered low emission and sustainable alternative to commercial fossil fuels. In the early stage of biogas reforming, CO_2-modified duckweed-obtained biochar showed 25% and 82% conversion of CH_4 and CO_2, respectively [189].

3.5.4 Supercapacitors

As compared to conventional capacitors, the supercapacitor as an energy storage device has gained noticeable attention due to its high power density, higher chemical stability, quick charge and discharge ability, and long life cycle [190]. Electrode material plays an outstanding role to determine the performance of energy storage devices. The ideal electrode of an energy storage device should possess a well-developed porous structure, higher surface area and excellent electrical conductivity, and its structural composition provides sufficient active sites for electrochemical oxidation. The common electrode material such as graphite granule, carbon nanotubes, graphene and activated carbon possess limited application due to its higher cost. Compared to the above material, the activated biochar–based electrode material has a higher surface area, porous structure and cost-effective, environmentally friendly material and therefore it exerts high electrical conductivity with a superior pseudo-capacitance. Acid-activated biochar as an electrode material can enhance the surface

oxygenated functional groups, which results in increasing the pseudo-capacitance [191]. Jiang et al. [192] have reported that the capacitance of woody biomass–obtained biochar has been increased from 14 to 115 F/g after nitric acid activation. The KOH-treated microporous-modified biochar at high activation temperature 675 °C showed higher capacitance between 220 and 245 F/g respectively [142]. Similarly, the NaOH-modified pine waste biochar generates a moderate specific capacitance (74 F/g at 20 mV/s) due to the high pore volume and large surface area of resulting biochar [193]. Biochar activation with metals can significantly improve the electrochemical performance of energy storage devices. Carbon aerogels activated with MnO_2 and Ni^{2+} were shown the more stable electrochemical performance and high power density, due to the treatment of electrochemically active metals and their large surface area [194]. Recently, Jiang et al. [195] tested the CO_2-activated biochar as electrode material in a supercapacitor cell and recorded a maximum current density of 100 mA/g and a specific capacitance of 80.9 F/g, respectively. The obtained results show that engineered pore structure, microporous structure, tortuous porous structure and surface functional groups were achieved through CO_2 activation, which is most beneficial to improve the electrochemical performance as well as the storage of ions in supercapacitor.

3.5.5 Fuel cell

The fuel cell is an electrochemical device that converts the chemical energy of fuel into electricity. It exhibits higher energy conversion efficiency and also reduces the greenhouse gas emission if green fuels are used. Recently, the direct carbon fuel cell (DCFC) is a robust device for the conversion of molten carbonaceous material into electricity through electrochemical oxidation that has been made by using coal- and corn cob–derived biochar in a direct carbon fuel cell [196]. Xiong et al. [197] found the better electrochemical performance of almond shell biochar in DCFC, and recorded peak power density of 127 m W cm^{-2}, which is comparatively higher than activated carbon fuel, i.e. 100 m W cm^{-2}. The electrochemical performance of fuel cells is mainly influenced by the physicochemical properties of biochar such as its chemical composition, surface oxygen functional groups, surface area and nature of mineral matter. A DCFC using activated biochar produces a relatively higher current (64.2 mA/cm^2) and power density of 32.8 mW/cm^2 at 0.5 V than commercial carbon black and hard coal about 55 mA/cm^2 and 28 mW/cm^2 at 0.5 V [198].

4 Conclusion

The conversion of organic biomass waste to biochar via a thermochemical process provides a new window for the environmentally sustainable management of waste. To improve the physicochemical properties of biochar for sustainable application, different activation methods might be selected. These activation methods, especially chemical activation, can improve the surface properties of biochar. Both acid and alkali activation can generate extensive functional groups while simultaneously modifying the surface area of the biochar. Alkali activation generates higher surface aromaticity and N/C ratios. The use of an oxidising agent or acid activation can increase the number of oxygen-containing functional groups on the biochar surface. However, impregnated biochar, despite its minimal pore volume, can increase the absorption capacities of organic and inorganic contaminants, along with improving their catalytic capacities. In summary, activated biochar has a wide platform for practical promotion in the field of environmental sustainability.

Compliance with ethical standards

Conflict of interest The authors declare that there is no conflict of interest.

References

1. Ahmed MB, Zhou JL, Ngo HH, Guo W (2015) Adsorptive removal of antibiotics from water and wastewater: progress and challenges. Sci Total Environ 532:112–126

2. Mohan D, Sarswat A, Ok YS, Pittman CU Jr (2014) Organic and inorganic contaminants removal from water with biochar, a renewable, low cost and sustainable adsorbent–a critical review. Bioresour Technol 160:191–202

3. Ahmad M, Rajapaksha AU, Lim JE, Zhang M, Bolan N, Mohan D, Vithanage M, Lee SS, Ok YS (2014) Biochar as a sorbent for contaminant management in soil and water: a review. Chemosphere 99:19–33

4. Novak JM, Lima I, Xing B et al (2009) Characterization of designer biochar produced at different temperatures and their effects on a loamy sand. Ann Environ Sci 3:195–206

5. Vithanage M, Rajapaksha AU, Ahmad M, Uchimiya M, Dou X, Alessi DS, Ok YS (2015) Mechanisms of antimony adsorption onto soybean stover-derived biochar in aqueous solutions. J Environ Manag 151:443–449

6. Ma Y, Liu WJ, Zhang N, Li YS, Jiang H, Sheng GP (2014) Polyethylenimine modified biochar adsorbent for hexavalent chromium removal from the aqueous solution. Bioresour Technol 169:403–408

7. Wang MC, Sheng GD, Qiu YP (2015) A novel manganese-oxide/biochar composite for efficient removal of lead (II) from aqueous solutions. Int J Environ Sci Technol 12:1719–1726

8. Tan X, Liu Y, Zeng G, Wang X, Hu X, Gu Y, Yang Z (2015) Application of biochar for the removal of pollutants from aqueous solutions. Chemosphere 125:70–85

9. Shen W, Li Z, Liu Y (2008) Surface chemical functional groups modification of porous carbon. Recent Patents on Chem Eng 1:27–40

10. Cha JS, Park SH, Jung SC, Ryu C, Jeon JK, Shin MC, Park YK (2016) Production and utilization of biochar: a review. J Ind Eng Chem 40:1–15

11. Collard FX, Blin J (2014) A review on pyrolysis of biomass constituents: mechanisms and composition of the products obtained from the conversion of cellulose, hemicelluloses and lignin. Renew Sust Energ Rev 38:594–608

12. Downie AE, Van Zwieten L, Smernik RJ et al (2011) Terra Preta Australis: reassessing the carbon storage capacity of temperate soils. Agric Ecosyst Environ 140:137–147

13. Huggins TM, Haeger A, Biffinger JC, Ren ZJ (2016) Granular biochar compared with activated carbon for wastewater treatment and resource recovery. Water Res 94:225–232

14. Tan G, Sun W, Xu Y, Wang H, Xu N (2016) Sorption of mercury (II) and atrazine by biochar, modified biochars and biochar based activated carbon in aqueous solution. Bioresour Technol 211:727–735

15. Nair V, Vinu R (2016) Peroxide-assisted microwave activation of pyrolysis char for adsorption of dyes from wastewater. Bioresour Technol 216:511–519

16. Yao Y, Gao B, Chen JJ, Yang L (2013) Engineered biochar reclaiming phosphate from aqueous solutions: mechanisms and potential application as a slowrelease fertilizer. Environ Sci Technol 47:8700–8708

17. Delgado LF, Charles P, Glucina K et al (2012) The removal of endocrine disrupting compounds, pharmaceutically activated compounds and cyanobacterial toxins during drinking water preparation using activated carbon—a review. Sci Total Environ 435:509–525

18. Sevilla M, Mokaya R (2014) Energy storage applications of activated carbons: supercapacitors and hydrogen storage. Energy Environ Sci 7:1250–1280

19. Shafeeyan MS, Daud WMAW, Houshmand A, Shamiri A (2010) A review on surface modification of activated carbon for carbon dioxide adsorption. J Anal Appl Pyrolysis 89:143–151

20. Lee HW, Kim YM, Kim S et al (2018) Review of the use of activated biochar for energy and environmental applications. Carbon Lett (Carbon Lett) 26:1–10

21. Ahmad M, Lee SS, Lim JE, Lee SE, Cho JS, Moon DH, Hashimoto Y, Ok YS (2014) Speciation and phytoavailability of lead and antimony in a small arms range soil amended with mussel shell, cow bone and biochar: EXAFS spectroscopy and chemical extractions. Chemosphere 95:433–441

22. Wang J, Zhuan R, Chu L (2019) The occurrence, distribution and degradation of antibiotics by ionizing radiation: an overview. Sci Total Environ 646:1385–1397

23. Zhang K, Sun P, Zhang Y (2019) Decontamination of Cr (VI) facilitated formation of persistent free radicals on rice husk derived biochar. Front Environ Sci Eng 13:22

24. Kalinke C, Oliveira PR, Oliveira GA, Mangrich AS, Marcolino-Junior LH, Bergamini MF (2017) Activated biochar: preparation, characterization and electroanalytical application in an alternative strategy of nickel determination. Anal Chim Acta 983:103–111

25. Adhikari S, Sajib S (2020) Effect of pyrolysis methods on physical properties of activated biochar and its application as cathode electrode for lithium-sulfur battery. Trans ASABE 63:485–493

26. Xiao Y, Zhang A, Liu S, Zhao J, Fang S, Jia D, Li F (2012) Free-standing and porous hierarchical nanoarchitectures constructed with cobalt cobaltite nanowalls for supercapacitors with high specific capacitances. J Power Sources 219:140–146

27. Ahn SY, Eom SY, Rhie YH, Sung YM, Moon CE, Choi GM, Kim DJ (2013) Utilization of wood biomass char in a direct carbon fuel cell (DCFC) system. Appl Energy 105:207–216

28. Alonso DM, Wettstein SG, Dumesic JA (2012) Bimetallic catalysts for upgrading of biomass to fuels and chemicals. Chem Soc Rev 41:8075–8098

29. Yahya MA, Al-Qodah Z, Ngah CZ (2015) Agricultural bio-waste materials as potential sustainable precursors used for activated carbon production: a review. Renew Sust Energ Rev 46:218–235

30. Roman S, Nabais JV, Ledesma B et al (2013) Production of low-cost adsorbents with tunable surface chemistry by conjunction of hydrothermal carbonization and activation processes. Microporous Mesoporous Mater 165:127–133

31. Mui EL, Cheung WH, Valix M et al (2010) Activated carbons from bamboo scaffolding using acid activation. Sep Purif Technol 74:213–218

32. Petkovic LM, Ginosar DM, Rollins HW et al (2009) Activated carbon catalysts for the production of hydrogen via the sulfur–iodine thermochemical water splitting cycle. Int J Hydrog Energy 34:4057–4064

33. Sha Y, Lou J, Bai S, Wu D, Liu B, Ling Y (2015) Facile preparation of nitrogen-doped porous carbon from waste tobacco by a simple pre-treatment process and their application in electrochemical capacitor and CO2 capture. Mater Res Bull 64:327–332

34. Htwe WM, Kyawt YY, Thaikua S, Imai Y, Mizumachi S, Kawamoto Y (2016) Effects of liming on dry biomass, lead concentration and accumulated amounts in roots and shoots of three tropical pasture grasses from lead contaminated acidic soils. Grassl Sci 62:257–261

35. Gautam RK, Mudhoo A, Lofrano G, Chattopadhyaya MC (2014) Biomass-derived biosorbents for metal ions sequestration: adsorbent modification and activation methods and adsorbent regeneration. J Environ Chem Eng 2:239–259

36. Acemioğlu B (2019) Removal of a reactive dye using NaOH-activated biochar prepared from peanut shell by pyrolysis process. Int J Coal Prep Util 1–23. https://doi.org/10.1080/19392699.2019.1644326

37. Mohammed J, Nasri NS, Zaini MA et al (2015) Adsorption of benzene and toluene onto KOH activated coconut shell based carbon treated with NH3. Int Biodeterior Biodegradation 102:245–255

38. Yang W, Liu Y, Wang Q, Pan J (2017) Removal of elemental mercury from flue gas using wheat straw chars modified by Mn-Ce mixed oxides with ultrasonic-assisted impregnation. Chem Eng J 326:169–181

39. Hamza UD, Nasri NS, Amin NS et al (2016) Characteristics of oil palm shell biochar and activated carbon prepared at different carbonization times. Desalin Water Treat 57:7999–8006

40. Adinaveen T, Kennedy LJ, Vijaya JJ et al (2015) Surface and porous characterization of activated carbon prepared from pyrolysis of biomass (rice straw) by two-stage procedure and its applications in supercapacitor electrodes. J Mater Cycles Waste Manag 17:736–747

41. Köseoğlu E, Akmil-Başar C (2015) Preparation, structural evaluation and adsorptive properties of activated carbon from agricultural waste biomass. Adv Powder Technol 26:811–818

42. Ozdemir I, Şahin M, Orhan R, Erdem M (2014) Preparation and characterization of activated carbon from grape stalk by zinc chloride activation. Fuel Process Technol 125:200–206

43. Tiryaki B, Yagmur E, Banford A, Aktas Z (2014) Comparison of activated carbon produced from natural biomass and equivalent chemical compositions. J Anal Appl Pyrolysis 105:276–283

44. Uysal T, Duman G, Onal Y, Yasa I, Yanik J (2014) Production of activated carbon and fungicidal oil from peach stone by two-stage process. J Anal Appl Pyrolysis 108:47–55

45. Largitte L, Brudey T, Tant T, Dumesnil PC, Lodewyckx P (2016) Comparison of the adsorption of lead by activated carbons from three lignocellulosic precursors. Microporous Mesoporous Mater 219:265–275

46. Hosseini S, Soltani SM, Jahangirian H et al (2015) Fabrication and characterization porous carbon rod-shaped from almond natural fibers for environmental applications. J Environ Chem Eng 3:2273–2280

47. Erabee IK, Ahsan A, Daud NN et al (2017) Manufacture of low-cost activated carbon using sago palm bark and date pits by physiochemical activation. Bioresources 12:1916–1923

48. Pallarés J, González-Cencerrado A, Arauzo I (2018) Production and characterization of activated carbon from barley straw by physical activation with carbon dioxide and steam. Biomass Bioenergy 115:64–73

49. Choi GG, Oh SJ, Lee SJ, Kim JS (2015) Production of bio-based phenolic resin and activated carbon from bio-oil and biochar derived from fast pyrolysis of palm kernel shells. Bioresour Technol 178:99–107

50. Saygılı H, Güzel F (2016) High surface area mesoporous activated carbon from tomato processing solid waste by zinc chloride activation: process optimization, characterization and dyes adsorption. J Clean Prod 113:995–1004

51. Suhas PJM, Carrott MML, Carrott R (2007) Lignin – from natural adsorbent to activated carbon: a review. Bioresour Technol 98:2301–2312

52. Zhao Y, Fang F, Xiao HM, Feng QP, Xiong LY, Fu SY (2015) Preparation of pore-size controllable activated carbon fibers from bamboo fibers with superior performance for xenon storage. Chem Eng J 270:528–534

53. Foo KY, Hameed BH (2012) Coconut husk derived activated carbon via microwave induced activation: effects of activation agents, preparation parameters and adsorption performance. Chem Eng J 184:57–65

54. González PG, Pliego-Cuervo YB (2013) Physicochemical and microtextural characterization of activated carbons produced from water steam activation of three bamboo species. J Anal Appl Pyrolysis 99:32–39

55. González-García P, Centeno TA, Urones-Garrote E, Ávila-Brande D, Otero-Díaz LC (2013) Microstructure and surface properties of lignocellulosic-based activated carbons. Appl Surf Sci 265:731–737

56. Abioye AM, Ani FN (2015) Recent development in the production of activated carbon electrodes from agricultural waste biomass for supercapacitors: a review. Renew Sust Energ Rev 52:1282–1293

57. Lua AC, Lau FY, Guo J (2006) Influence of pyrolysis conditions on pore development of oil-palm-shell activated carbons. J Anal Appl Pyrolysis 76:96–102

58. Ioannidou O, Zabaniotou A (2007) Agricultural residues as precursors for activated carbon production—a review. Renew Sust Energ Rev 11:1966–2005

59. Uchimiya M, Chang S, Klasson KT (2011) Screening biochars for heavy metal retention in soil: role of oxygen functional groups. J Hazard Mater 190:432–441

60. Park JH, Ok YS, Kim SH, Cho JS, Heo JS, Delaune RD, Seo DC (2015) Evaluation of phosphorus adsorption capacity of sesame straw biochar on aqueous solution: influence of activation methods and pyrolysis temperatures. Environ Geochem Health 37:969–983

61. Vithanage M, Rajapaksha AU, Zhang M, Thiele-Bruhn S, Lee SS, Ok YS, Thiele-Bruhn S, Lee SS, Ok YS (2015) Acid-activated biochar increased sulfamethazine retention in soils. Environ Sci Pollut Res 22:2175–2186

62. Zhao B, O'Connor D, Zhang J, Peng T, Shen Z, Tsang DCW, Hou D (2018) Effect of pyrolysis temperature, heating rate, and residence time on rapeseed stem derived biochar. J Clean Prod 174:977–987

63. Al-Wabel MI, Al-Omran A, El-Naggar AH et al (2013) Pyrolysis temperature induced changes in characteristics and chemical composition of biochar produced from conocarpus wastes. Bioresour Technol 131:374–379

64. González PG (2018) Activated carbon from lignocellulosics precursors: a review of the synthesis methods, characterization techniques and applications. Renew Sust Energ Rev 82:1393–1414

65. Ali I (2010) The quest for active carbon adsorbent substitutes: inexpensive adsorbents for toxic metal ions removal from wastewater. Sep Purif Rev 39:95–171

66. Chen Y, Zhu Y, Wang Z, Li Y, Wang L, Ding L, Gao X, Ma Y, Guo Y (2011) Application studies of activated carbon derived from rice husks produced by chemical-thermal process—a review. Adv Colloid Interf Sci 163:39–52

67. Puziy AM, Poddubnaya OI, Martınez-Alonso A et al (2002) Characterization of synthetic carbons activated with phosphoric acid. Appl Surf Sci 200:196–202

68. Hadjittofi L, Prodromou M, Pashalidis I (2014) Activated biochar derived from cactus fibres–preparation, characterization and application on Cu (II) removal from aqueous solutions. Bioresour Technol 159:460–464

69. Giraldo L, Moreno-Pirajan JC (2012) Synthesis of activated carbon mesoporous from coffee waste and its application in adsorption zinc and mercury ions from aqueous solution. J Chemother 9:938–948

70. Dutta S, Kim J, Ide Y, Ho Kim J, Hossain MSA, Bando Y, Yamauchi Y, Wu KCW (2017) 3D network of cellulose-based energy storage devices and related emerging applications. Mater Horiz 4:522–545. https://doi.org/10.1039/C6MH00500D

71. Lukatskaya MR, Dunn B, Gogotsi Y (2016) Multidimensional materials and device architectures for future hybrid energy storage. Nat Commun 7:12647. https://doi.org/10.1038/ncomms12647

72. Xu G, Nie P, Dou H et al (2017) Exploring metal organic frameworks for energy storage in batteries and supercapacitors. Mater Today 20:191–209

73. Bardestani R, Kaliaguine S (2018) Steam activation and mild air oxidation of vacuum pyrolysis biochar. Biomass Bioenergy 108:101–112

74. Vijayaraghavan K (2019) Recent advancements in biochar preparation, feedstocks, modification, characterization and future applications. Environ Technol Rev 8:47–64

75. Rajapaksha AU, Vithanage M, Ahmad M, Seo DC, Cho JS, Lee SE, Lee SS, Ok YS (2015) Enhanced sulfamethazine removal by steam-activated invasive plant-derived biochar. J Hazard Mater 290:43–50

76. Chakraborty P, Banerjee S, Kumar S, Sadhukhan S, Halder G (2018) Elucidation of ibuprofen uptake capability of raw and steam activated biochar of Aegle marmelos shell: isotherm, kinetics, thermodynamics and cost estimation. Process Saf Environ Prot 118:10–23

77. Sewu DD, Jung H, Kim SS, Lee DS, Woo SH (2019) Decolorization of cationic and anionic dye-laden wastewater by steam-activated biochar produced at an industrial-scale from spent mushroom substrate. Bioresour Technol 277:77–86

78. Xiao F, Pignatello JJ (2015) Interactions of triazine herbicides with biochar: steric enhanced sulfamethazine removal by steam-activated invasive plant-derived biochar. J Hazard Mater 90:43–50

79. Abu Bakar MS (2019) Comparison of chemical properties and adsorption capabilities of different pyrolysis temperature biochar and steam activated biochar derived from empty fruit bunch (EFB).

80. Olivares-Marín M, Fernández-González C, Macías-García A, Gómez-Serrano V (2012) Preparation of activated carbon from cherry stones by physical activation in air. Influence of the chemical carbonisation with H2SO4. J Anal Appl Pyrolysis 94:131–137

81. Ould-Idriss A, Stitou M, Cuerda-Correa EM, Fernández-González C, Macías-García A, Alexandre-Franco MF, Gómez-Serrano V (2011) Preparation of activated carbons from olive-tree wood revisited. II Physical activation with air. Fuel Process Technol 92:266–270

82. Kwiatkowski M, Broniek E (2017 Sep 20) An analysis of the porous structure of activated carbons obtained from hazelnut shells by various physical and chemical methods of activation. Colloids Surf A Physicochem Eng Asp 529:443–453

83. Shao J, Zhang J, Zhang X, Feng Y, Zhang H, Zhang S, Chen H (2018) Enhance SO2 adsorption performance of biochar modified by CO2 activation and amine impregnation. Fuel 224:138–146

84. Xiong Z, Shihong Z, Haiping Y, Tao S, Yingquan C, Hanping C (2013) Influence of NH 3/CO 2 modification on the characteristic of biochar and the CO 2 capture. BioEnergy Res 6:1147–1153

85. Zhang X, Zhang S, Yang H, Feng Y, Chen Y, Wang X, Chen H (2014) Nitrogen enriched biochar modified by high temperature CO2–ammonia treatment: characterization and adsorption of CO2. Chem Eng J 257:20–27

86. Qian K, Kumar A, Zhang H, Bellmer D, Huhnke R (2015) Recent advances in utilization of biochar. Renew Sust Energ Rev 42: 1055–1064

87. Aghababaei A, Ncibi MC, Sillanpää M (2017) Optimized removal of oxytetracycline and cadmium from contaminated waters using chemically-activated and pyrolyzed biochars from forest and wood-processing residues. Bioresour Technol 239:28–36

88. Issa AA, Al-Degs YS, El-Sheikh AH et al (2017) Application of partial least squares-kernel calibration in competitive adsorption studies using an effective chemically activated biochar. CLEAN–Soil Air Water 45:1600333

89. Hsu D, Lu C, Pang T, Wang Y, Wang G (2019) Adsorption of ammonium nitrogen from aqueous solution on chemically activated biochar prepared from sorghum distillers grain. Appl Sci 9: 5249

90. Braghiroli FL, Bouafif H, Neculita CM et al (2019) Performance of physically and chemically activated biochars in copper removal from contaminated mine effluents. Water Air Soil Pollut 230:178

91. Yin Q, Ren H, Wang R et al (2018) Evaluation of nitrate and phosphate adsorption on Al-modified biochar: influence of Al content. Sci Total Environ 631:895–903

92. Jin J, Li S, Peng X, Liu W, Zhang C, Yang Y, Han L, du Z, Sun K, Wang X (2018) HNO3 modified biochars for uranium (VI) removal from aqueous solution. Bioresour Technol 256:247–253

93. Liu P, Liu WJ, Jiang H, Chen JJ, Li WW, Yu HQ (2012) Modification of bio-char derived from fast pyrolysis of biomass and its application in removal of tetracycline from aqueous solution. Bioresour Technol 121:235–240

94. Rajapaksha AU, Chen SS, Tsang DC et al (2016) Engineered/ designer biochar for contaminant removal/immobilization from soil and water: potential and implication of biochar modification. Chemosphere 148:276–291

95. Ippolito JA, Ducey TF, Cantrell KB, Novak JM, Lentz RD (2016) Designer, acidic biochar influences calcareous soil characteristics. Chemosphere 142:184–191

96. Peng P, Lang YH, Wang XM (2016) Adsorption behavior and mechanism of pentachlorophenol on reed biochars: pH effect, pyrolysis temperature, hydrochloric acid treatment and isotherms. Ecol Eng 90:225–233

97. Cao L, Iris KM, Tsang DC et al (2018) Phosphoric acid-activated wood biochar for catalytic conversion of starch-rich food waste into glucose and 5-hydroxymethylfurfural. Bioresour Technol 267:242–248

98. Cordero-Lanzac T, Hita I, Veloso A, Arandes JM, Rodríguez-Mirasol J, Bilbao J, Cordero T, Castaño P (2017) Characterization and controlled combustion of carbonaceous deactivating species deposited on an activated carbon-based catalyst. Chem Eng J 327:454–464

99. Hita I, Cordero-Lanzac T, Gallardo A, Arandes JM, Rodríguez-Mirasol J, Bilbao J, Cordero T, Castaño P (2016) Phosphorus-containing activated carbon as acid support in a bifunctional Pt–Pd catalyst for tire oil hydrocracking. Catal Commun 78:48–51

100. García-Mateos FJ, Berenguer R, Valero-Romero MJ, Rodríguez-Mirasol J, Cordero T (2018) Phosphorus functionalization for the rapid preparation of highly nanoporous submicron-diameter carbon fibers by electrospinning of lignin solutions. J Mater Chem A 6:1219–1233

101. Peng H, Gao P, Chu G et al (2017) Enhanced adsorption of Cu (II) and Cd (II) by phosphoric acid-modified biochars. Environ Pollut 229:846–853

102. Iriarte-Velasco U, Sierra I, Zudaire L et al (2016) Preparation of a porous biochar from the acid activation of pork bones. Food Bioprod Process 98:341–353

103. Lei S, Dongmei C, Shungang W, Zebin Y et al (2015) Performance, kinetics, and equilibrium of methylene blue adsorption on biochar derived from eucalyptus saw dust modified with citric, tartaric, and acetic acids. Bioresour Technol 198:300–308

104. Sun K, Tang J, Gong Y et al (2015) Characterization of potassium hydroxide (KOH) modified hydrochars from different feedstocks for enhanced removal of heavy metals from water. Environ Sci Pollut Res 22:16640–16651

105. Zhang X, Zhang L, Li A (2018) Eucalyptus sawdust derived biochar generated by combining the hydrothermal carbonization and low concentration KOH modification for hexavalent chromium removal. J Environ Manag 206:989–998

106. Cazetta (2011)

107. Mosa AA, El-Ghamry A, Al-Zahrani H et al (2017) Chemically modified biochar derived from cotton stalks: characterization And assessing its potential for heavy metals removal from wastewater. Environ Biodiv Soil Secur 1:33–45

108. Hu X, Xue Y, Long L et al (2018) Characteristics and batch experiments of acid-and alkali-modified corncob biomass for nitrate removal from aqueous solution. Environ Sci Pollut Res 25:19932–19940

109. Hasnan FI, Iamail KN, Musa M et al (2018) Characterization of bio char derived from tapioca skin. In: IOP Conference Series: Materials Science and Engineering, vol 334, pp 012–016

110. Shen Y, Zhang N (2019) Facile synthesis of porous carbons from silica-rich rice husk char for volatile organic compounds (VOCs) sorption. Bioresour Technol 282:294–300

111. Trakal L, Vítková M, Hudcová B et al (2019) Biochar and its composites for metal (loid) removal from aqueous solutions. In: Biochar from Biomass and Waste, pp 113–141

112. Wang S, Gao B, Zimmerman AR et al (2015) Removal of arsenic by magnetic biochar prepared from pinewood and natural hematite. Bioresour Technol 175:391–395

113. Wang P, Tang L, Wei X et al (2017) Synthesis and application of iron and zinc doped biochar for removal of p-nitrophenol in wastewater and assessment of the influence of co-existed Pb (II). Appl Surf Sci 392:391–401

114. Liang J, Fang Y, Luo Y et al (2019) Magnetic nanoferromanganese oxides modified biochar derived from pine sawdust for adsorption of tetracycline hydrochloride. Environ Sci Pollut Res 26:5892–5903

115. Tang N, Niu C, Li X et al (2018) Efficient removal of Cd2+ and Pb2+ from aqueous solution with amino- and thiol-functionalized activated carbon: isotherm and kinetics modeling. Sci Total Environ 635:1331–1344

116. Akgül G, Maden TB, Diaz E et al (2019) Modification of tea biochar with Mg, Fe, Mn and Al salts for efficient sorption of PO43− and Cd2+ from aqueous solutions. J Water Reuse Desalin 9:57–66

117. Wang Z, Wu J, He T et al (2014) Corn stalks char from fast pyrolysis as precursor material for preparation of activated carbon in fluidized bed reactor. Bioresour Technol 167:551–554

118. Niksiar A, Nasernejad B (2017) Activated carbon preparation from pistachio shell pyrolysis and gasification in a spouted bed reactor. Biomass Bioenergy 106:43–50

119. Carrier M, Hardie AG, Uras U et al (2012) Production of char from vacuum pyrolysis of South-African sugar cane bagasse and

its characterization as activated carbon and biochar. J Anal Appl Pyrolysis 96:24–32

120. Tripathi M, Sahu JN, Ganesan P (2016) Effect of process parameters on production of biochar from biomass waste through pyrolysis: a review. Renew Sust Energ Rev 55:467–481

121. Brown AB. Development and utilization of a Raman characterization method for Hydrothermal char 2019

122. Jiang SF, Sheng GP, Jiang H (2019) Advances in the characterization methods of biomass pyrolysis products. ACS Sustain Chem Eng 7:12639–12655

123. Wang J, Liao Z, Ifthikar J et al (2017) One-step preparation and application of magnetic sludge-derived biochar on acid orange 7 removal via both adsorption and persulfate based oxidation. RSC Adv **7**:18696–18706

124. Yoo S, Kelley S, Tilotta D et al (2018) Structural characterization of loblolly pine derived biochar by x-ray diffraction and electron energy loss spectroscopy. ACS Sustain Chem Eng 6:2621–2629

125. Zhao Y, Feng D, Zhang Y et al (2016) Effect of pyrolysis temperature on char structure and chemical speciation of alkali and alkaline earth metallic species in biochar. Fuel Process Technol 141:54–60

126. Igalavithana AD, Mandal S, Niazi NK et al (2017) Advances and future directions of biochar characterization methods and applications. Crit Rev Environ Sci Technol 47:2275–2330

127. Intani K, Latif S, Cao Z et al (2018) Characterisation of biochar from maize residues produced in a self-purging pyrolysis reactor. Bioresour Technol 265:224–235

128. Shim T, Yoo J, Ryu C et al (2015) Effect of steam activation of biochar produced from a giant Miscanthus on copper sorption and toxicity. Bioresour Technol 197:85–90

129. Rajapaksha AU, Vithanage M, Lee SS et al (2016) Steam activation of biochars facilitates kinetics and pH-resilience of sulfamethazine sorption. J Soils Sediments 16:889–895.103

130. Wang RZ, Huang DL, Liu YG et al (2019) Synergistic removal of copper and tetracycline from aqueous solution by steam-activated bamboo-derived biochar. J Hazard Mater 384:121470

131. Franciski MA, Peres EC, Godinho M et al (2018) Development of CO2 activated biochar from solid wastes of a beer industry and its application for methylene blue adsorption. Waste Manag 78:630–638

132. Vaughn SF, Kenar JA, Tisserat B et al (2017) Chemical and physical properties of Paulownia elongata biochar modified with oxidants for horticultural applications. Ind Crop Prod 97:260–267

133. Taskin MB, Kadioglu YK, Sahin O et al (2019) Effect of acid modified biochar on the growth and essential and non-essential element content of bean, chickpea, soybean, and maize grown in calcareous soil. Commun Soil Sci Plant Anal 1–10:105

134. Huff MD, Lee JW (2016) Biochar-surface oxygenation with hydrogen peroxide. J Environ Manag 165:17–21

135. Güzel F, Sayğılı H, Sayğılı GA et al (2017) Optimal oxidation with nitric acid of biochar derived from pyrolysis of weeds and its application in removal of hazardous dye methylene blue from aqueous solution. J Clean Prod 144:260–265

136. Zhang D, Li Y, Sun A et al (2019) Enhanced nitrobenzene reduction by modified biochar supported sulfidated nano zerovalent iron: comparison of surface modification methods. Sci Total Environ 694: 133701

137. El-Khateeb A, Al-Zahrani H, Selim EM et al (2017) Chemically modified biochar derived from cotton stalks: characterization and assessing its potential for heavy metals removal from wastewater. electronic effects. Water Res 80:179–188

138. Ding Z, Hu X, Wan Y et al (2016) Removal of lead, copper, cadmium, zinc, and nickel from aqueous solutions by alkali-modified biochar: batch and column tests. J Ind Eng Chem 33:239–245

139. Jin HM, Capared S, Chang ZZ et al (2014) Biochar pyrolytically produced from municipal solid wastes for aqueous As(V) removal: sorption property and its improvement with KOH activation. Bioresour Technol 169:622–629

140. Li B, Yang L, Wang CQ et al (2017) Adsorption of Cd (II) from aqueous solutions by rape straw biochar derived from different modification processes. Chemosphere 175:332–340

141. He R, Yuan X, Huang Z et al (2019) Activated biochar with iron-loading and its application in removing Cr (VI) from aqueous solution. Colloids Surf A Physicochem Eng Asp 579:123642

142. Dehkhoda AM, Gyenge E, Ellis N et al (2016) A novel method to tailor the porous structure of KOH-activated biochar and its application in capacitive deionization and energy storage. Biomass Bioenergy 87:107–121

143. Ding S, Liu Y (2020) Adsorption of CO2 from flue gas by novel seaweed-based KOH-activated porous biochars. Fuel 260:116–382

144. Duan XL, Yuan CG, Jing TT et al (2019) Removal of elemental mercury using large surface area micro-porous corn cob activated carbon by zinc chloride activation. Fuel 239:830–840

145. Park JH, Ok YS, Kim SH et al (2015) Competitive adsorption of heavy metals onto sesame straw biochar in aqueous solutions. Chemosphere 142:77–83

146. Naeem MA, Imran M, Amjad M (2019) Batch and column scale removal of cadmium from water using raw and acid activated wheat straw biochar. Water 11:1438

147. Zhu L, Zhao N, Tong L (2018) Structural and adsorption characteristics of potassium carbonate activated biochar. RSC Adv 8: 21012–21019

148. Jung C, Boateng LK, Flora JR et al (2015) Competitive adsorption of selected non-steroidal anti-inflammatory drugs on activated biochars: experimental and molecular modeling study. Chem Eng J 264:1–9

149. Li C, Zhang L, Gao Y et al (2018) Facile synthesis of nano ZnO/ZnS modified biochar by directly pyrolyzing of zinc contaminated corn stover for Pb (II), Cu (II) and Cr (VI) removals. Waste Manag 79:625–637

150. Wang S, Gao B, Li Y et al (2015) Manganese oxide-modified biochars: preparation, characterization, and sorption of arsenate and lead. Bioresour Technol 181:13–17

151. Gan C, Liu Y, Tan X et al (2015) Effect of porous zinc–biochar nanocomposites on Cr (VI) adsorption from aqueous solution. RSC Adv 5:35107–35115

152. Wang H, Gao B, Wang S et al (2015) Removal of Pb (II), Cu (II), and Cd (II) from aqueous solutions by biochar derived from KMnO4 treated hickory wood. Bioresour Technol 197:356–362

153. Trakal L, Veselská V, Šafařík I et al (2016) Lead and cadmium sorption mechanisms on magnetically modified biochars. Bioresour Technol 203:318–324

154. Fan Z, Zhang Q, Li M et al (2018) Investigating the sorption behavior of cadmium from aqueous solution by potassium permanganate-modified biochar: quantify mechanism and evaluate the modification method. Environ Sci Pollut Res 25:8330–8339

155. Zhou L, Huang Y, Qiu W et al (2017) Adsorption properties of nano-MnO2–biochar composites for copper in aqueous solution. Molecules 22:173

156. Jiang D, Chu B, Amano Y et al (2018) Removal and recovery of phosphate from water by Mg-laden biochar: batch and column studies. Colloids Surf A Physicochem Eng Asp 558:429–437

157. Li H, Dong X, da Silva EB et al (2017) Mechanisms of metal sorption by biochars: biochar characteristics and modifications. Chemosphere 178:466–478

158. Yu J, Jiang C, Guan Q et al (2018) Enhanced removal of Cr (VI) from aqueous solution by supported ZnO nanoparticles on biochar derived from waste water hyacinth. Chemosphere 195:632–640

159. Han Y, Cao X, Ouyang X et al (2016) Adsorption kinetics of magnetic biochar derived from peanut hull on removal of Cr (VI) from aqueous solution: effects of production conditions and particle size. Chemosphere 145:336–341

160. Li R, Wang JJ, Zhou B et al (2017) Simultaneous capture removal of phosphate, ammonium and organic substances by MgO

impregnated biochar and its potential use in swine wastewater treatment. J Clean Prod 147:96–107

161. O'Connor D, Peng T, Li G et al (2018) Sulfur-modified rice husk biochar: a green method for the remediation of mercury contaminated soil. Sci Total Environ 621:819–826

162. Villalobos M, Escobar-Quiroz IN, Salazar-Camacho C (2014) The influence of particle size and structure on the sorption and oxidation behavior of birnessite: I. Adsorption of As (V) and oxidation of As (III). Geochim Cosmochim Acta 125:564–581

163. Yu Z, Zhou L, Huang Y et alEffects of a manganese oxide-modified biochar composite on adsorption of arsenic in red soil. J Environ Manag 163:155–162

164. Zhang F, Wang X, Xionghui J et al (2016) Efficient arsenate removal by magnetite-modified water hyacinth biochar. Environ Pollut 216:575–583

165. Lu K, Yang X, Gielen G et al (2017) Effect of bamboo and rice straw biochars on the mobility and redistribution of heavy metals (Cd, Cu, Pb and Zn) in contaminated soil. J Environ Manag 186:285–292

166. Liu H, Xu F, Xie Y et al (2018) Effect of modified coconut shell biochar on availability of heavy metals and biochemical characteristics of soil in multiple heavy metals contaminated soil. Sci Total Environ 645:702–709

167. Frick H, Tardif S, Kandeler E et al (2019) Assessment of biochar and zero-valent iron for in-situ remediation of chromated copper arsenate contaminated soil. Sci Total Environ 655:414–422

168. Moon DH, Hwang I, Chang YY et al (2017) Quality improvement of acidic soils by biochar derived from renewable materials. Environ Sci Pollut Res 24:4194–4199

169. Lin L, Li Z, Liu X et al (2019) Effects of Fe-Mn modified biochar composite treatment on the properties of As-polluted paddy soil. Environ Pollut 244:600–607

170. Cerino-Córdova FJ, Díaz-Flores PE, García-Reyes RB et al (2013) Biosorption of Cu (II) and Pb (II) from aqueous solutions by chemically modified spent coffee grains. Int J Environ Sci Technol 10:611–622

171. Yan L, Kong L, Qu Z et al (2015) Magnetic biochar decorated with ZnS nanocrytals for Pb (II) removal. ACS Sustain Chem Eng 3:125–132

172. Agrafioti E, Kalderis D, Diamadopoulos E (2014) Ca and Fe modified biochars as adsorbents of arsenic and chromium in aqueous solutions. J Environ Manag 146:444–450

173. Son EB, Poo KM, Chang JS et al (2018) Heavy metal removal from aqueous solutions using engineered magnetic biochars derived from waste marine macro-algal biomass. Sci Total Environ 615:161–168

174. Li Y, Shao J, Wang X et al (2014) Characterization of modified biochars derived from bamboo pyrolysis and their utilization for target component (furfural) adsorption. Energy Fuel 28:5119–5127

175. Sun L, Chen D, Wan S et al (2015) Performance, kinetics, and equilibrium of methylene blue adsorption on biochar derived from eucalyptus saw dust modified with citric, tartaric, and acetic acids. Bioresour Technol 198:300–308

176. Chen B, Chen Z, Lv S (2011) A novel magnetic biochar efficiently sorbs organic pollutants and phosphate. Bioresour Technol 102:716–723

177. Ahmad M, Lee SS, Rajapaksha AU et al (2013) Trichloroethylene adsorption by pine needle biochars produced at various pyrolysis temperatures. Bioresour Technol 143:615–622

178. Zhang XN, Mao GY, Jiao YB et al (2014) Adsorption of anionic dye on magnesium hydroxide-coated pyrolytic bio-char and reuse by microwave irradiation. Int J Environ Sci Technol 11:1439–1448

179. Mubarak NM, Kundu A, Sahu JN et al (2014) Synthesis of palm oil empty fruit bunch magnetic pyrolytic char impregnating with FeCl3 by microwave heating technique. Biomass Bioenergy 61:265–275

180. Wu JW, Wu CR, Zhou CS et al (2020) Fate and removal of antibiotic resistance genes in heavy metals and dye co-contaminated wastewater treatment system amended with β-cyclodextrin functionalized biochar. Sci Total Environ 723:1–8

181. Jing XR, Wang YY, Liu WJ et al (2014) Enhanced adsorption performance of tetracycline in aqueous solutions by methanol-modified biochar. Chem Eng J 248:168–174

182. Lee J, Kim KH, Kwon EE (2017) Biochar as a catalyst. Renew Sust Energ Rev 77:70–79

183. Zhang X, Tong J, Hu BX et al (2018) Adsorption and desorption for dynamics transport of hexavalent chromium (Cr (VI)) in soil column. Environ Sci Pollut Res 25:459–468

184. Tian K, Liu WJ, Zhang S et al (2016) One-pot synthesis of a carbon supported bimetallic Cu–Ag NPs catalyst for robust catalytic hydroxylation of benzene to phenol by fast pyrolysis of biomass waste. Green Chem 18:5643–5650

185. Zhao C, Lv P, Yang L et al (2018) Biodiesel synthesis over biochar-based catalyst from biomass waste pomelo peel. Energy Convers Manag 160:477–485

186. Zhao C, Yang L, Xing S et al (2018) Biodiesel production by a highly effective renewable catalyst from pyrolytic rice husk. J Clean Prod 199:772–780

187. Shen Y, Zhao P, Shao Q et al (2014) In-situ catalytic conversion of tar using rice husk char-supported nickel-iron catalysts for biomass pyrolysis/gasification. Appl Catal B Environ 152:140–151

188. Swierczynski D, Libs S, Courson C et al (2007) Steam reforming of tar from a biomass gasification process over Ni/olivine catalyst using toluene as a model compound. Appl Catal B Environ 74:211–222

189. Muradov N, Fidalgo B, Gujar AC et al (2012) Production and characterization of Lemna minor bio-char and its catalytic application for biogas reforming. Biomass Bioenergy 42:123–131

190. Wang L, Wang Y, Ma F et al (2019) Mechanisms and reutilization of modified biochar used for removal of heavy metals from wastewater: a review. Sci Total Environ 668:1298–1309

191. Qian K, Kumar A, Zhang H et al (2015) Recent advances in utilization of biochar. Renew Sust Energ Rev 42:1055–1064

192. Jiang J, Zhang L, Wang X et al (2013) Highly ordered macroporous woody biochar with ultra-high carbon content as supercapacitor electrodes. Electrochim Acta 113:481–489

193. He N, Yoo S, Meng J et al (2017) Engineering biorefinery residues from loblolly pine for supercapacitor applications. Carbon. 120:304–312

194. Wang Y, Wang Y, Jiang L (2018) Freestanding carbon aerogels produced from bacterial cellulose and its Ni/MnO 2/Ni (OH) 2 decoration for supercapacitor electrodes. J Appl Electrochem 48:495–507

195. Jiang C, Yakaboylu GA, Yumak T et al (2020) Activated carbons prepared by indirect and direct CO2 activation of lignocellulosic biomass for supercapacitor electrodes. Renew Energy 20:1–41

196. Yu J, Zhao Y, Li Y (2014) Utilization of corn cob biochar in a direct carbon fuel cell. J Power Sources 270:312–317

197. Xiong X, Iris KM, Cao L et al (2017) A review of biochar-based catalysts for chemical synthesis, biofuel production, and pollution control. Bioresour Technol 246:254–270

198. Kacprzak A, Kobyłecki R, Włodarczyk R et al (2014) The effect of fuel type on the performance of a direct carbon fuel cell with molten alkaline electrolyte. J Power Sources 255:179–186